Sedimentology (2002) **49,** 669–695

Turbidite depositional architecture across three interconnected deep-water basins on the north-west African margin

RUSSELL B. WYNN, PHILIP P. E. WEAVER, DOUGLAS G. MASSON and DORRIK A. V. STOW
Southampton Oceanography Centre, European Way, Southampton SO14 3ZH, UK (E-mail: rbw1@soc.soton.ac.uk)

ABSTRACT

The Moroccan Turbidite System (MTS) on the north-west African margin extends 1500 km from the head of the Agadir Canyon to the Madeira Abyssal Plain, making it one of the longest turbidite systems in the world. The MTS consists of three interconnected deep-water basins, the Seine Abyssal Plain (SAP), the Agadir Basin and the Madeira Abyssal Plain (MAP), connected by a network of distributary channels. Excellent core control has enabled individual turbidites to be correlated between all three basins, giving a detailed insight into the turbidite depositional architecture of a system with multiple source areas and complex morphology. Large-volume (> 100 km^3) turbidites, sourced from the Morocco Shelf, show a relatively simple architecture in the Madeira and Seine Abyssal Plains. Sandy bases form distinct lobes or wedges that thin rapidly away from the basin margin and are overlain by ponded basin-wide muds. However, in the Agadir Basin, the turbidite fill is more complex owing to a combination of multiple source areas and large variations in turbidite volume. A single, very large turbidity current (200–300 km^3 of sediment) deposited most of its sandy load within the Agadir Basin, but still had sufficient energy to carry most of the mud fraction 500 km further downslope to the MAP. Large turbidity currents (100–150 km^3 of sediment) deposit most of their sand and mud fraction within the Agadir Basin, but also transport some of their load westwards to the MAP. Small turbidity currents (< 35 km^3 of sediment) are wholly confined within the Agadir Basin, and their deposits pinch out on the basin floor. Turbidity currents flowing beyond the Agadir Basin pass through a large distributary channel system. Individual turbidites correlated across this channel system show major variations in the mineralogy of the sand fraction, whereas the geochemistry and micropalaeontology of the mud fraction remain very similar. This is interpreted as evidence for separation of the flow, with a sand-rich, erosive, basal layer confined within the channel system, overlain by an unconfined layer of suspended mud. Large-volume turbidites within the MTS were deposited at oxygen isotope stage boundaries, during periods of rapid sea-level change and do not appear to be specifically connected to sea-level lowstands or highstands. This contrasts with the classic fan model, which suggests that most turbidites are deposited during lowstands of sea level. In addition, the three largest turbidites on the MAP were deposited during the largest fluctuations in sea level, suggesting a link between the volume of sediment input and the magnitude of sea-level change.

Keywords Sediment cores, turbidites, turbidity currents.

INTRODUCTION AND AIMS

The north-west African continental margin has for many years been the focus of intensive research into modern deep-water sedimentary processes. For example, on the Madeira Abyssal Plain (MAP), a total of over 160 sediment cores has been recovered (Fig. 1), allowing detailed correlation of the late Quaternary turbidite sequence (Weaver & Rothwell, 1987; Rothwell *et al.*, 1992; Weaver *et al.*, 1992). In addition, the timing and source area of turbidites on the MAP has been investi-

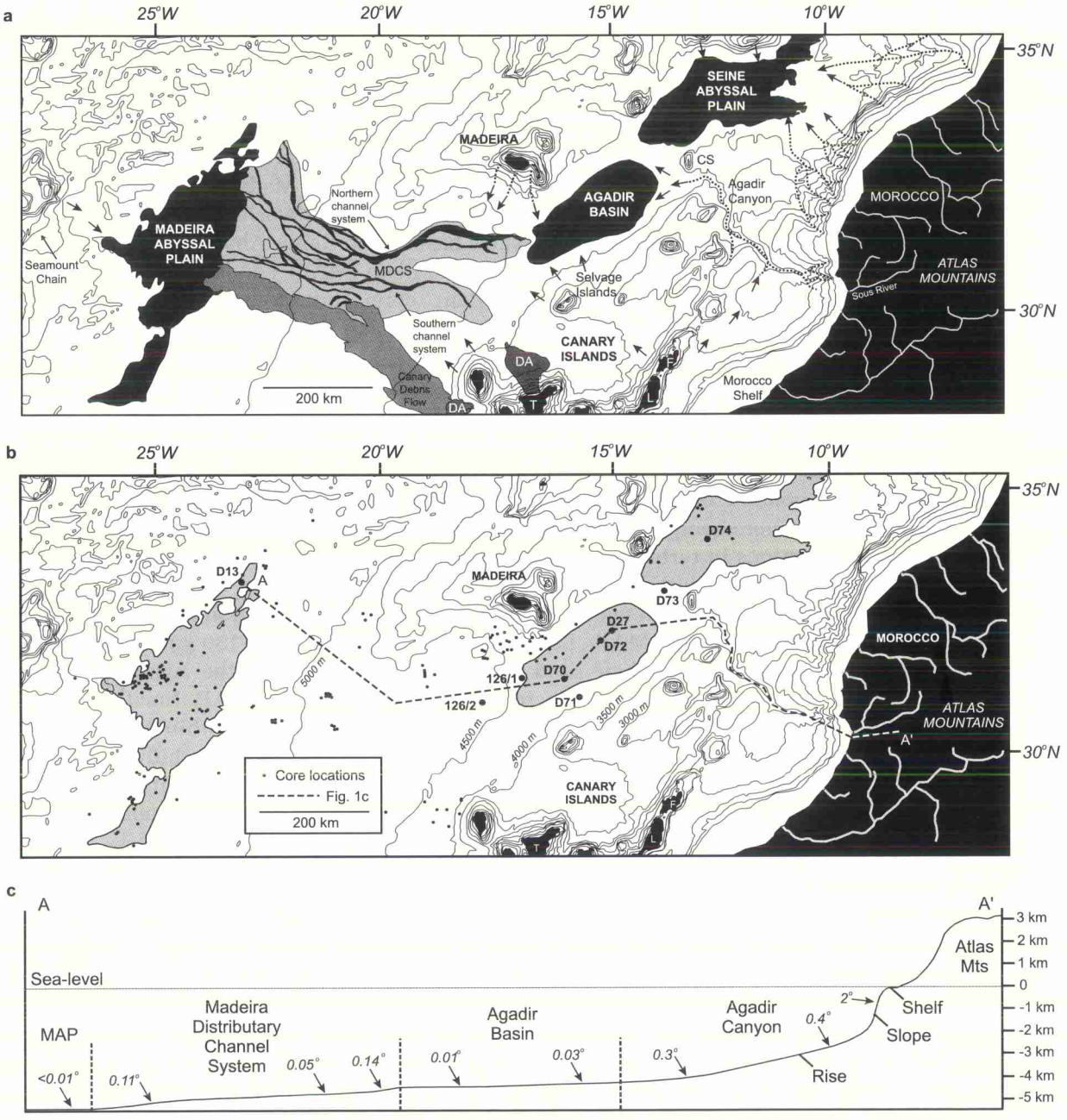

Fig. 1. (a) Location map showing the main features of the Moroccan Turbidite System (MTS). Principal transport directions for turbidity currents are shown by arrows and dashed lines. CS, Casablanca Seamount; DA, debris avalanche; MDCS, Madeira Distributary Channel System; T, Tenerife; L, Lanzarote; F, Fuerteventura. (b) Map showing all core locations within the study area. The nine cores used in this study are indicated, as is the location of the line of cross-section shown in (c). Bathymetric contours spaced at 500-m intervals. (c) Cross-section A–A′ showing the variations in slope angle across the MTS. Note the change in gradient between the almost flat Agadir Basin and the head of the MDCS.

gated in detail, revealing that turbidites deposited since the mid-Miocene are sourced from three main areas: the north-west African margin, the volcanic Canary Islands and seamounts to the west of the plain (Figs 1 and 2) (Weaver & Kuijpers, 1983; de Lange *et al.*, 1987; Pearce & Jarvis, 1992; Weaver *et al.*, 1998). Additional research by Masson (1994), Davies *et al.* (1997), and Ercilla *et al.* (1998) has provided some insight into the transport direction of turbidites derived from the Moroccan margin and Canary Islands. However, a more detailed knowledge of turbidity current pathways onto the MAP from these source areas has only recently been established (Weaver *et al.*, 2000; Wynn *et al.*, 2000). A major pathway for turbidites derived from the Moroccan margin and Canary Islands can now be traced from source to sink and has been termed the Moroccan Turbidite System (MTS).

Long run-out turbidite systems, in which turbidity currents travel over distances >800 km, have been recognized in several of the world's oceans (e.g. Laurentian Fan, Piper *et al.*, 1984; Amazon Fan, Damuth & Flood, 1985; Bengal Fan, Emmel & Curray, 1985; Indus Fan, Kolla & Coumes, 1985; north-west Atlantic Mid-Ocean Channel, Hesse *et al.*, 1987, 1996; Hikurangi Channel, Lewis, 1994; Zaire Fan, Droz *et al.*, 1996). In the MTS, turbidity currents transport sediments derived from the Atlas Mountains up to 1500 km before deposition on the MAP, making this one of the longest turbidite systems in the world (Wynn *et al.*, 2000). However, unlike most other long run-out systems, the MTS has been extensively cored throughout its length, and individual turbidites can be correlated across a distance of 1200 km. This gives an unprecedented insight into the proximal-to-distal variations in depositional architecture of turbidites within a long run-out system. The MTS is also unique because, in this topographically complex area, turbidity currents derived from one source can deposit a single turbidite across three different interconnected basins. The excellent core control in this area therefore also provides new insights into the distribution and thickness of sand bodies in a turbidite system with complex sea-floor topography.

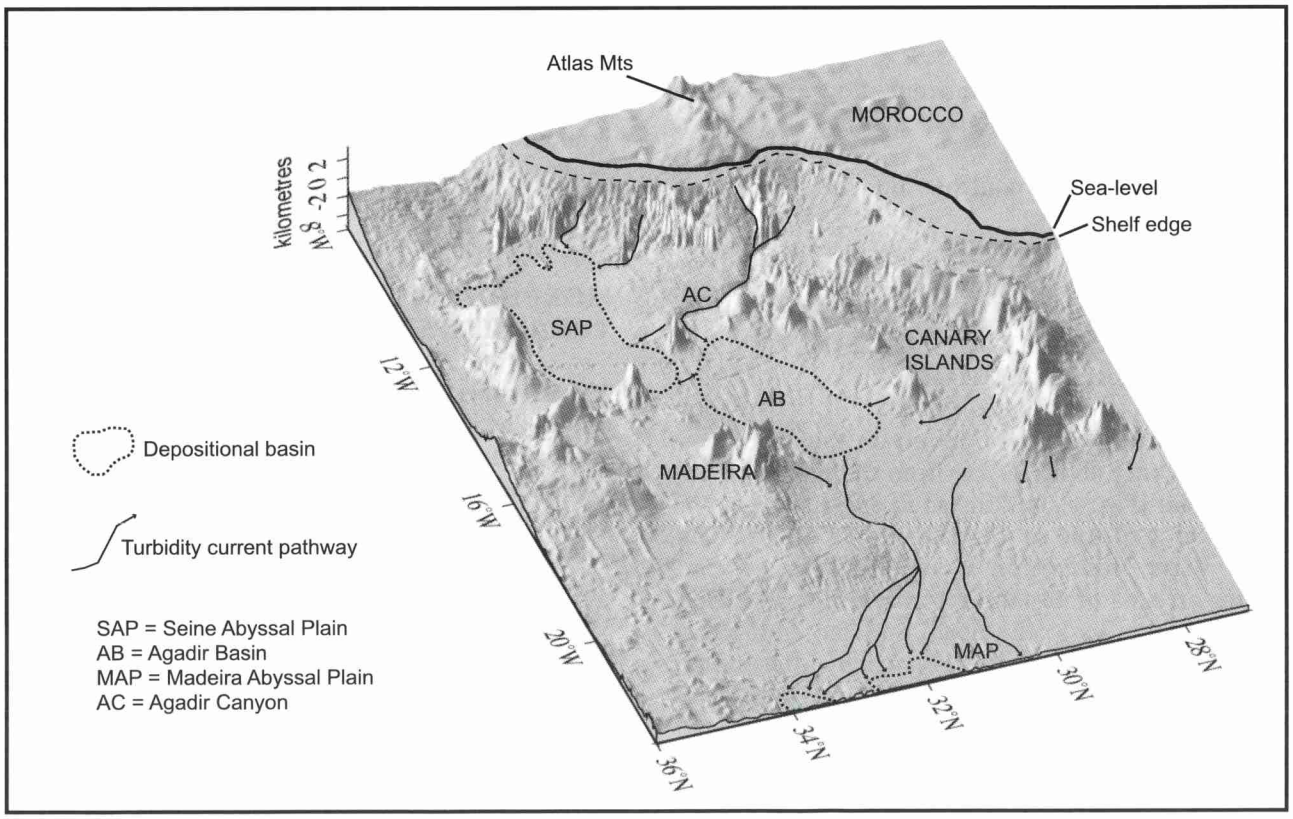

Fig. 2. Grey-shaded three-dimensional map of the MTS, showing the Agadir Canyon (AC), Seine Abyssal Plain (SAP), Agadir Basin (AB) and the eastern edge of the Madeira Abyssal Plain (MAP). The topography above sea level was constructed using the ETOPO5 database, and the submarine bathymetry was constructed using ship track data.

Therefore, the principal aims of this study are to:

1 correlate individual turbidites between three different depositional basins within the MTS and identify the turbidite source areas. This is achieved by first describing and correlating the turbidite sequence in a series of new piston cores collected from across the Agadir Basin and its margins. The correlated Agadir Basin sequence is then tied into single representative cores from the MAP and Seine Abyssal Plain (SAP). These single cores will themselves be tied into the well-established turbidite sequences on the MAP and SAP, as described previously by Weaver *et al.* (1992) and Davies (1995). The end-result is correlation of the turbidite sequence in three different depositional basins. A combination of five techniques (sand fraction composition, magnetic susceptibility, turbidite colour, micropalaeontological dating and relative stratigraphic position) are used in turbidite correlation and source area identification.

2 use the correlated sequence across all three basins to examine the turbidite depositional architecture within the MTS from source to sink, with particular emphasis on sand body distribution and lateral variations in turbidite thickness and grain size.

3 interpret turbidity current flow processes using a combination of sedimentary structures and mineralogical data.

4 investigate the controls on the timing of turbidite deposition.

COASTAL AND ONSHORE GEOLOGY, GEOMORPHOLOGY AND CLIMATE OF THE AGADIR REGION

The head of the Agadir Canyon on the Moroccan margin is only about 35 km from the mouth of the Sous River (Fig. 1), and the shelf edge is at a water depth of 110–150 m (Ercilla *et al.*, 1998). The Sous River lies within a synclinal valley that drains an area of 16 000 km^2, including the High Atlas Mountains to the north and the Anti-Atlas Mountains to the south. The High Atlas range consists of Palaeozoic and Mesozoic sediments that were uplifted and folded during the mid- to late Tertiary. The Anti-Atlas Mountains consist of uplifted Palaeozoic metasediments and Precambrian igneous and metamorphic rocks (Summerhayes *et al.*, 1976). The Sous Valley receives annual rainfall of 200–400 mm, and adjacent areas of the High Atlas receive 400–800 mm. This is considerably higher than the arid hinterland south of the Anti-Atlas, where annual rainfall is only 25–50 mm. The Sous River is one of the few major rivers on this margin that is perennial in its lower reaches, and is therefore associated with a higher rate of terrigenous flux (Griffiths, 1972; Summerhayes *et al.*, 1976). Historical records from the last 700 years suggest that the Agadir region is still being affected by ongoing tectonic activity in the form of earthquakes, and this may also contribute to the offshore transport of terrigenous material (McMaster & Lachance, 1969; Akil & Gayet, 1988).

The composition of shelf sediments is affected by the close proximity of the Sous River, which supplies terrigenous sediments derived from the adjacent mountain ranges. The outer shelf and upper slope is covered by coarse sands, dominantly containing shells, foraminifera, glauconite and quartz (McMaster & Lachance, 1969). The inner and mid-shelf is covered by a belt of silts and muds that is absent from the more sediment-starved areas to the north and south. These sediments are characterized by a lower carbonate content than adjacent areas, reflecting the increased terrigenous input. The sediments also have higher illite:smectite, chlorite:kaolinite and amphibole:pyroxene ratios than adjacent areas, confirming their source as the metamorphic and igneous complexes of the Atlas and Anti-Atlas ranges (Summerhayes *et al.*, 1976; Jaaidi & Cirac, 1987; Akil & Gayet, 1988).

MORPHOLOGY OF THE MOROCCAN TURBIDITE SYSTEM

The Moroccan Turbidite System (MTS) originates on the Moroccan margin, before running westwards between the Canary and Madeira archipelagos and terminating on the MAP (Figs 1 and 2). The MTS has a total length of 1500 km, and its morphology is largely controlled by the position of volcanic islands, seamounts and salt diapirs (Wynn *et al.*, 2000). The MTS has been classified as a 'turbidity current pathway' (Wynn *et al.*, 2000), although it could also be argued that it is a morphologically complex form of elongate fan (e.g. Stow, 1985; Reading & Richards, 1994). It is longitudinally extended perpendicular to the Moroccan margin, has a broad head region at the top of the main Agadir Canyon, a complex distributary channel system and large terminal

lobes constructed at channel terminations on the MAP. However, the complex morphology of the MTS is responsible for additional features not accounted for by standard fan models, such as the location of the 'intraslope' Agadir Basin and the multiple input points.

The MTS can be subdivided into five main morphological segments: the Agadir Canyon, the Agadir Basin, the Seine Abyssal Plain, the Madeira Distributary Channel System and the Madeira Abyssal Plain.

The Agadir Canyon lies at the edge of the northern Morocco Shelf, offshore from the termination of the Sous River, which drains the High Atlas hinterland (Fig. 1). The canyon is 460 km long, 5–15 km wide and 600–1500 m deep and opens out onto the lower rise at a water depth of 4250 m before passing westwards into the flat-lying Agadir Basin (Ercilla *et al.*, 1998).

The Agadir Basin is a large depositional basin with an area of 38 000 km^2 and a maximum water depth of 4450 m (Fig. 1). From the mouth of the Agadir Canyon to the western basin margin, the average gradient is just 0·02° (Fig. 1c). The Agadir Basin is separated from the Seine Abyssal Plain (SAP) to the north-east by an intrabasinal sill. This sill is >100 m above the height of the basin floor and is composed of interbedded turbidites and pelagic/hemipelagic sediments lying upon flat acoustic basement (Davies *et al.*, 1997). The Agadir Basin is bordered to the north and south by the volcanic archipelagos of the Madeira and Canary/Selvage Islands. At the western edge of the basin, the head of a broad distributary channel system correlates with a small increase in slope gradient.

The Madeira Distributary Channel System (MDCS) on the continental rise east of the MAP can be subdivided into two major channel systems. The northern channel system runs west from the edge of the Agadir Basin and then turns to the north-west before terminating on the north-east margin of the MAP; the southern channel system runs west-north-west from the submarine slopes of the Canary Islands before terminating on the eastern margin of the MAP (Masson, 1994; Fig. 1). Channel dimensions and spacing are strongly controlled by gradient (Fig. 1b and c). Broad, shallow channels, <10–20 m deep, occur in the central braided section of the channel system, on a slope of ≈0·05°. The deepest channels, which are up to 50 m deep, occur in the adjacent deeply incised sections, on slightly steeper slopes of 0·11–0·14° (Masson, 1994).

The Madeira Abyssal Plain (MAP) covers an area of 68 000 km^2, lies at a water depth of 5400 m and has an overall gradient of <0·01° (Searle, 1987; Rothwell *et al.*, 1992). The MAP marks the western limit for turbidites transported downslope along the MTS, as its western boundary is bordered by the Great Meteor–Hyeres–Cruiser seamount chain (Fig. 1).

DATA COLLECTION AND ANALYTICAL TECHNIQUES

This study primarily describes seven new giant piston cores collected from the Agadir Basin and its margins during research cruises on the *RRS Discovery* and *RRS Charles Darwin* in 1997 and 2001. These cores have been used to correlate the turbidite sequence across the Agadir Basin and its margins. In addition, a single new core (D74, Fig. 1b) was collected from the SAP during *RRS Discovery* cruise 225 in 1997. This core is also described in detail and correlated with the established SAP turbidite sequence (Davies, 1995). Another single core (D13, Fig. 1b) was collected from the MAP during *RRS Discovery* cruise 177 in 1988. This core has been described previously by Weaver *et al.* (1992), but has been redescribed and sampled in detail for this study and correlated with the established MAP turbidite sequence (e.g. Weaver *et al.*, 1992). The key characteristics of the nine cores are displayed in Table 1, and all core locations are shown in Fig. 1b.

Sedimentary logs were made of all cores, with careful attention paid to sediment colour, visual grain size and turbidite/hemipelagite/pelagite differentiation. In addition, the sedimentary structures of selected turbidites were logged in detail to enable interpretation of turbidity current processes. Multisensor core logging included magnetic susceptibility, which is particularly useful for determining the presence of volcanic components in sandy turbidite bases (e.g. Robinson, 1993).

Analysis of turbidite sand mineralogy was carried out in an attempt to understand more about the provenance of individual turbidites and as an aid to correlation. Approximately 1 cm^3 of sediment was sampled from each sandy turbidite base and bathed in 10% acetic acid. This removed the majority of the carbonate fraction, as only terrigenous clastic sediments were to be analysed. All samples were then wet sieved and divided into four grain size classes from 63 μm to >500 μm. The main mineral constituents in every

Table 1. Key characteristics of the nine cores used in this study.

Core no.	Core location (lat. + long.)	Environment	Depth (m)	Length (cm)	Turbidites per m	Turbidite/ pelagite ratio	Sand/mud ratio
D13	33°12′ N/23°30′ W	Madeira Abyssal Plain	5420	1000	0·9	92:8	13:87
CD126/1	31°27′ N/17°00′ W	Agadir Basin margin	4454	558	2·5	27:73	9:91
CD126/2	30°59′ N/18°00′ W	Lower continental rise	4566	519	1·3	48:52	28:72
D71	31°07′ N/15°51′ W	Lower continental rise	4311	1201	1·3	29:71	5:95
D70	31°30′ N/16°12′ W	Agadir Basin floor	4404	1061	1·2	71:29	16:84
D72	32°23′ N/15°17′ W	Agadir Basin floor	4365	801	1·4	51:49	19:81
D27	32°36′ N/15°00′ W	Agadir Basin floor	4358	376	2·1	44:56	16:84
D73	32°59′ N/13°57′ W	Between AB and SAP	4315	998	3·8	57:43	11:89
D74	34°00′ N/13°00′ W	Seine Abyssal Plain	4411	858	2·0	66:34	13:87

grain-size class were recorded, and 300 individual grains were point counted and identified for the following grain-size classes: very fine sand (63–125 μm); fine sand (125–250 μm); medium sand (250–500 μm); and coarse sand (> 500 μm).

A micropalaeontological technique developed by Weaver (1994) has been used for dating and correlation of turbidites in the cores. In this technique, the ratios of different species of coccoliths (calcareous algae) are analysed in both pelagic layers and the mud fraction of turbidites. This provides a stratigraphic framework and a method of correlating turbidites between cores.

1 The stratigraphic scheme uses both first and last appearance datum levels (FADs and LADs) and species abundance data (acmes). Coccoliths show a turnover of dominant species through the Quaternary, with a single species outnumbering all others for a few tens or hundreds of thousands of years before giving way to another dominant species (Thierstein *et al.*, 1977; Weaver, 1983). A combination of FADs, LADs and dominance intervals therefore provides a large number of coccolith datum levels in the late Quaternary. For example, within the Brunhes palaeomagnetic interval, there are six recognizable coccolith intervals (Weaver, 1993). The coccolith stratigraphy has been tied into the oxygen isotope stratigraphy (Weaver & Kuijpers, 1983; Martinson *et al.*, 1987), and it appears that most large turbidites in the MTS occur at oxygen isotope stage boundaries (Weaver & Kuijpers, 1983; Weaver *et al.*, 1992). It should be noted that there is a small potential error in calculating turbidite ages based upon coccolith ratios and oxygen isotope stage boundaries, relating to the amount of bioturbation and/or erosion present and the exact position of the turbidite relative to the oxygen isotope boundary (Weaver & Kuijpers, 1983). However, these factors are not easily quantifiable. Therefore, all turbidite ages quoted actually relate to the oxygen isotope stratigraphy and not to the exact age of turbidite emplacement. For example, a turbidite may have been deposited at the boundary between oxygen isotope stages five and six. This boundary has been dated precisely at 130 ka (Martinson *et al.*, 1987) and, therefore, implies that the turbidite was deposited at $\approx$130 ka.

2 The turbidite muds contain mixtures of coccoliths from more than one isotope stage, as the slope failure that initiated the turbidity current would have eroded some depth into the seabed.

Weaver (1994) showed that this mixture was relatively constant for each turbidite in a range of cores from across the whole MAP and, furthermore, that different turbidites had different coccolith mixtures. In this study, the coccolith mixtures within turbidite muds are used to aid correlation of turbidites both within and between basins.

A series of 3·5 kHz profiles across several core locations has been included to give an indication of the acoustic facies (Fig. 3). These profiles are the most important data set for the description of regional sediment facies distribution. A review of the echofacies characteristics on the north-west African margin is presented by Masson *et al.* (1992) and Wynn *et al.* (2000).

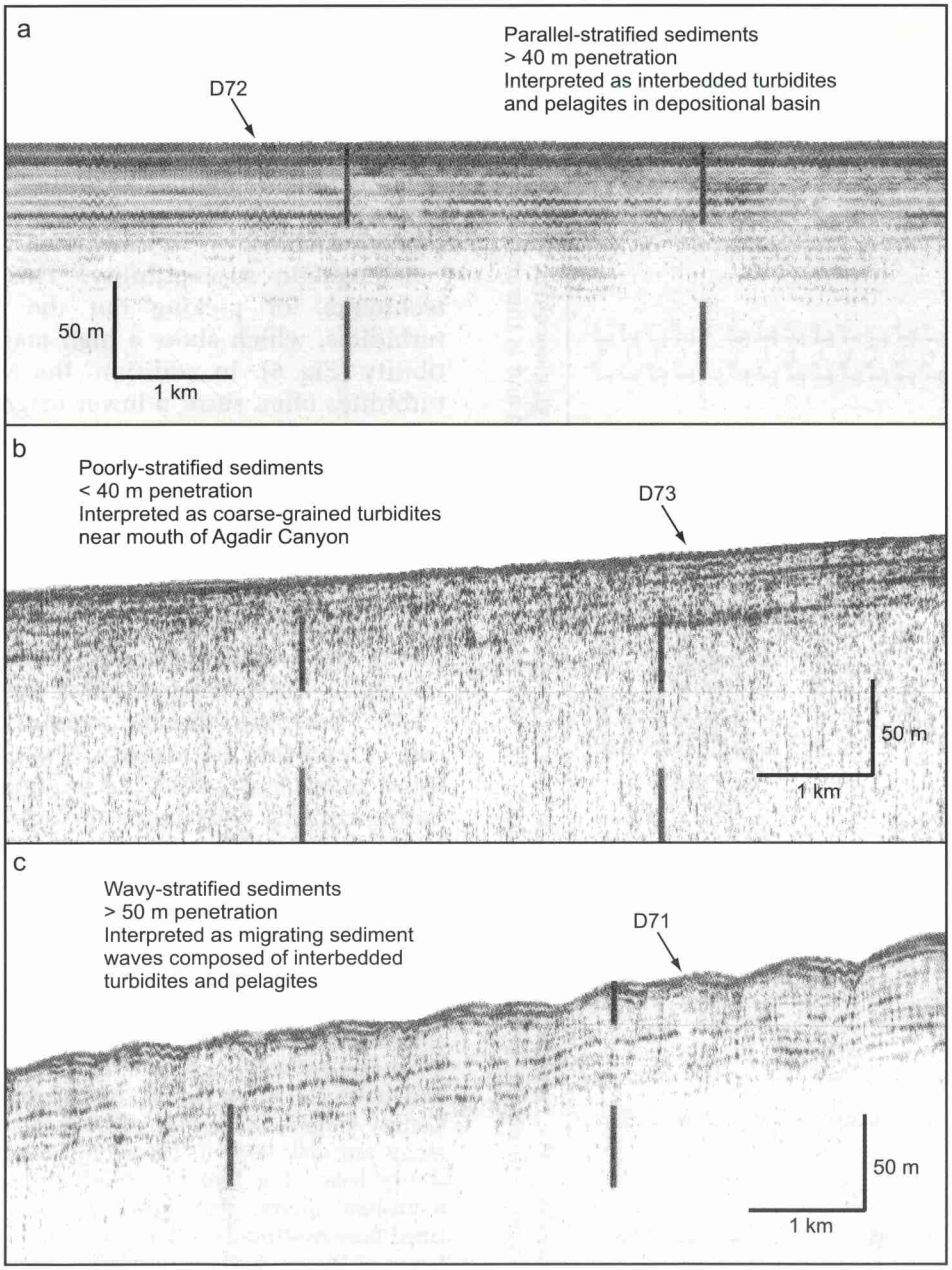

Fig. 3. A series of 3·5-kHz profiles showing the acoustic character of the sea floor at various core localities. (a) Typical basin-fill facies in the vicinity of core D72 and also typical of cores D13, D70, D27 and D74. (b) Proximal levee facies in the vicinity of core D73. (C) Migrating sediment wave facies in the vicinity of core D71. All core locations are shown in Fig. 1b. Vertical dashes across the figures are scale/time bars and do not represent actual data.

Table 2. Characteristics of individual turbidites in the Agadir Basin sequence and their interpreted source area.

Turbidite number	MAP quiv.	SAP equiv.	Max. thickness (cm) (sandy base)	Mud colour	Magnetic susc. (SI)	Bouma divisions	Erosive base	Sand fraction mineralogy	Interpreted source
1	a		34 (0)	Grey-green	15	T_e	No	NA	Canary Slope?
2	b		54 (1)	Grey-brown	40–240	T_a–T_e	Yes	VG, VL	West Canaries
3		d	24 (10)	Olive-green	15–20	T_a–T_e	Yes	Qz, ir ox, gl, CL, mi	Morocco Shelf
4			17 (0)	Grey-brown	20–30	T_d–T_e	No	NA	Canary Islands
5	d	e	177 (66)	Olive-grey	15–60	T_a–T_e	Yes	Qz, CL, gl, py, dol	Morocco Shelf
6		h	10 (7)	Brown (ox)	15–35	T_a–T_e	No	Qz, gl, CL, mi	Morocco Shelf
7	e		75 (11)	Olive-green	0–15	T_a–T_e	Yes	Qz, py, VG, spi, mi	East Canaries?
8			18 (6)	Grey	> 200	T_a–T_e	No	VL, VG, qz	Canary Islands
9			12 (0)	Olive-grey	15	T_d–T_e	No	NA	Morocco Shelf
10	e_1	i	46 (15)	Olive-green	5–20	T_a–T_e	Yes	Qz, gl, CL, mi, dol	Morocco Shelf
11		j	34 (0)	Olive-grey	0–15	T_e	No	NA	Morocco Shelf
12	f	k	135 (87)	Olive-green	15–50	T_a–T_e	Yes	Qz, gl, CL, mi, spi	Morocco Shelf
13		l	30 (7)	Olive-grey	10–15	T_a–T_e	No	Qz, mi, gl, CL	Morocco Shelf
14	g	m	151+ (50+)	Grey	60–290	T_a–T_e	Yes	VG, VL, qz, mi, spi	North Tenerife
15		n	32+ (3+)	Brown (ox)	15–40	T_a–T_e	Yes	Qz, mi, gl, CL, py	Morocco Shelf

Key for mineralogy: VG, volcanic glass; VL, volcanic lithics; Qz, quartz; ir ox, iron oxide; gl, glauconite; CL, clastic lithic; mi, mica; py, pyrite; dol, dolomite; spi, spicules. Under mud colour, (ox) means that the turbidite mud has been fully oxidized and is therefore not its original colour.

THE TURBIDITE SEQUENCE IN THE AGADIR BASIN

Detailed correlation of turbidites in the Agadir Basin, based upon the seven new cores, has been achieved using a combination of:

1 Turbidite colour. This is useful in assessing the source area of turbidites and can assist in visual correlation. Nearly all the turbidites derived from the Morocco Shelf have olive-green or olive-grey muddy tops, whereas the few Canary Island turbidites can easily be picked out because of their grey or grey-brown muddy tops (Table 2).

2 Sand fraction composition. The sandy turbidite bases often show a distinctive mineralogy (Figs 4 and 5). This mineralogical composition remains roughly similar for individual turbidites across the basin floor, making this a useful correlation tool.

3 Magnetic susceptibility. This is a useful technique for picking out the volcaniclastic turbidites, which show a high magnetic susceptibility (Fig. 6). In addition, the Morocco Shelf turbidites often show a lower magnetic susceptibility than the adjacent pelagic and hemipelagic sediments, and these distinctive intervals can easily be correlated.

4 Micropalaeontological dating. The pelagic stratigraphy of the Agadir Basin sequence has been established in two cores (D71 and D72) using coccolith analyses (Fig. 7) and is very similar to the well-documented coccolith stratigraphy of the MAP (Weaver, 1994) and SAP (Davies, 1995). This means that the Agadir Basin sequence can be tied into the oxygen isotope stratigraphy (Martinson *et al.*, 1987), which provides some dating control. This helps to improve the correlation both within the Agadir Basin and also between the Agadir Basin, MAP and SAP, as described later.

Fig. 4. Core photographs showing the sedimentary structures of two turbidites in the Agadir Basin. Turbidite *AB5*(*Md*) is sourced from the Morocco Shelf, and turbidite *AB14*(*Mg*) is sourced from the volcanic Canary Islands. Examples of the sand fraction mineralogy are also shown: (1) a typical sample from the sandy base of a Morocco Shelf turbidite containing abundant quartz, glauconite, clastic lithics and pyritized burrows/fossils; (2) a selection of grains from the bases of Morocco Shelf turbidites, including fish teeth and vertebrae, lignified wood, dolomite, mica and pyrite; (3) a typical sample from the base of a Canary Island turbidite, containing altered volcanic glass and lithic fragments.

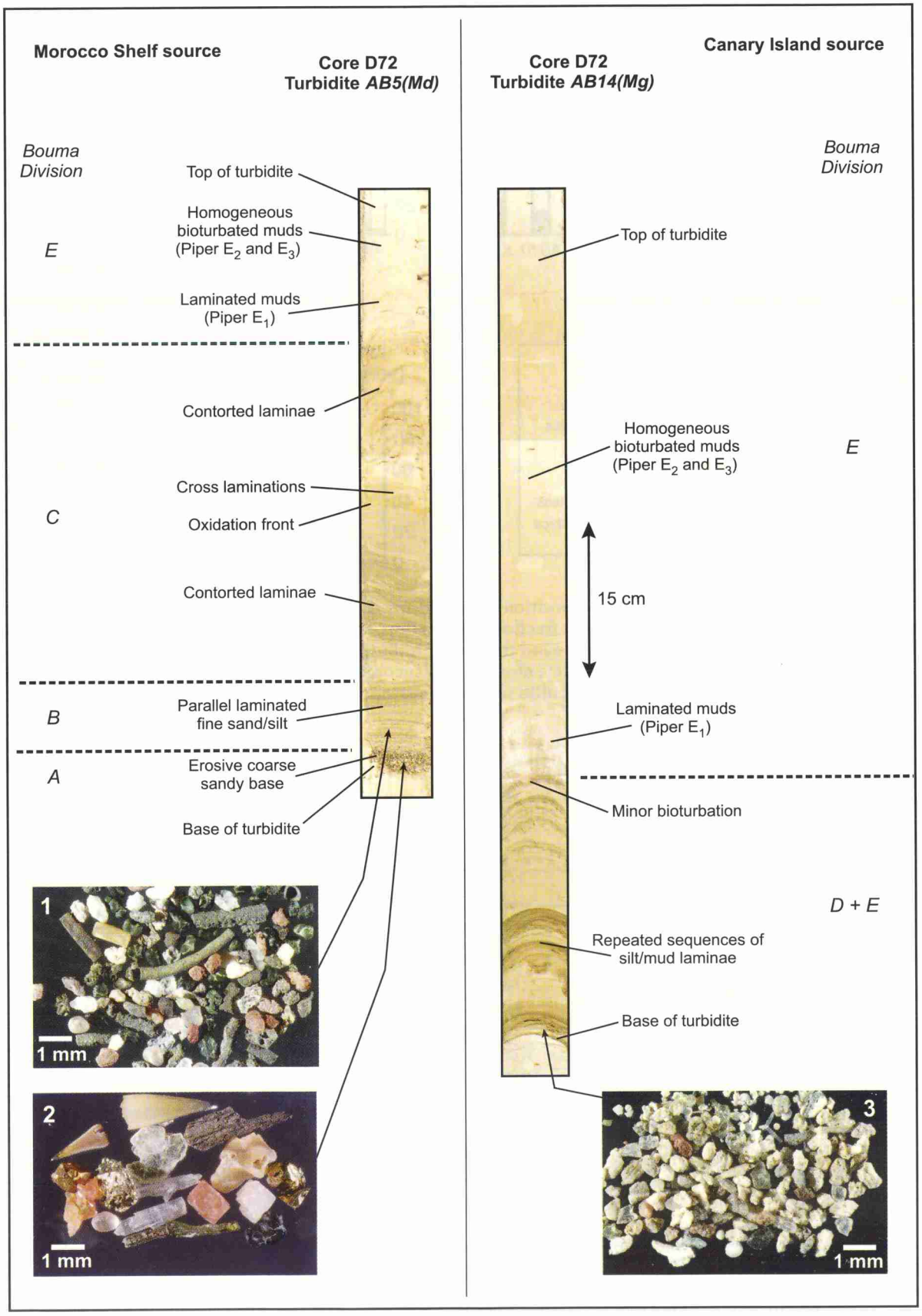
Morocco Shelf source
Core D72
Turbidite AB5(Md)
Bouma Division
Top of turbidite
Homogeneous bioturbated muds (Piper E2 and E3)
E
Laminated muds (Piper E1)
Contorted laminae
Cross laminations
C
Oxidation front
Contorted laminae
B
Parallel laminated fine sand/silt
A
Erosive coarse sandy base
Base of turbidite
1
1 mm
2
1 mm
Canary Island source
Core D72
Turbidite AB14(Mg)
Bouma Division
Top of turbidite
Homogeneous bioturbated muds (Piper E2 and E3)
E
15 cm
Laminated muds (Piper E1)
Minor bioturbation
D + E
Repeated sequences of silt/mud laminae
Base of turbidite
3
1 mm

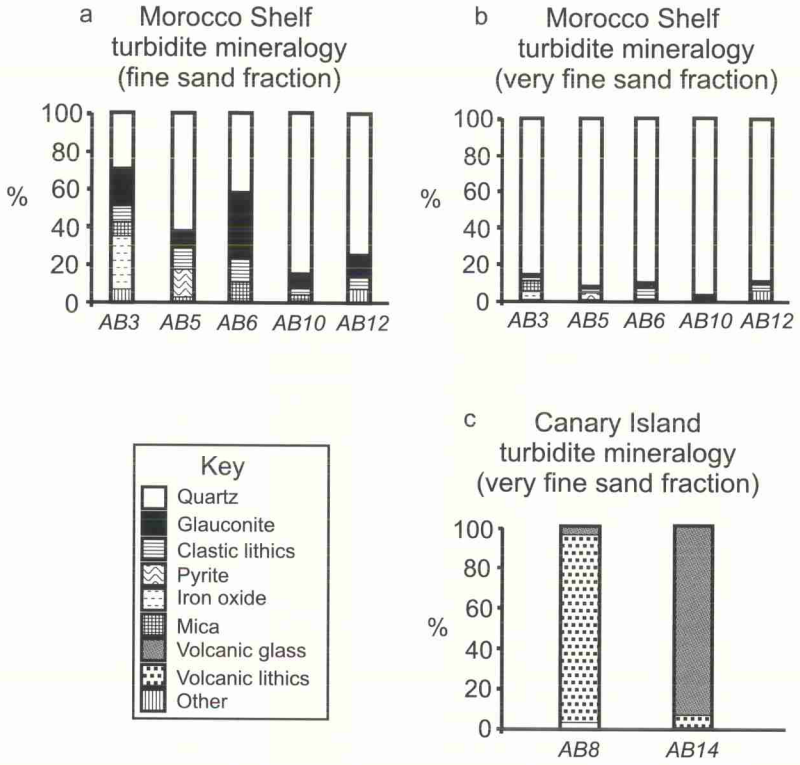

Fig. 5. Graphs showing the percentage composition of turbidites derived from (a) the Morocco Shelf (fine sand fraction), (b) the Morocco Shelf (very fine sand fraction) and (c) the Canary Islands (very fine sand fraction). Note the increased percentage of quartz in the very fine sand fraction of turbidites derived from the Morocco Shelf, compared with the fine sand fraction, and also the complete absence of glauconite and clastic lithics in turbidites derived from the Canary Islands. AB, Agadir Basin and turbidite numbers correspond to those shown in Fig. 8 and Table 2.

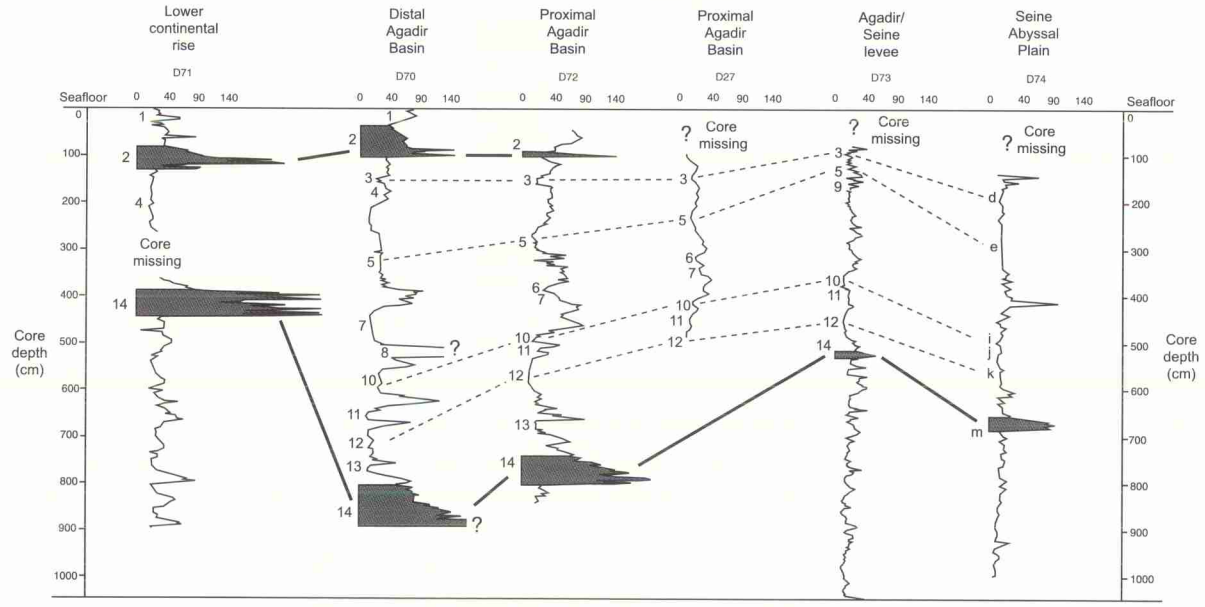

Fig. 6. Magnetic susceptibility logs for five Agadir Basin cores and one Seine Abyssal Plain core. Turbidite numbers or letters, as shown in Table 2, are indicated alongside the logs and can be correlated between cores. The high magnetic susceptibility values of the two large volcaniclastic turbidites (*AB2* and *AB14*) enable them to be picked out easily with dark grey shading. The horizontal scale on the magnetic susceptibility logs is in SI units.

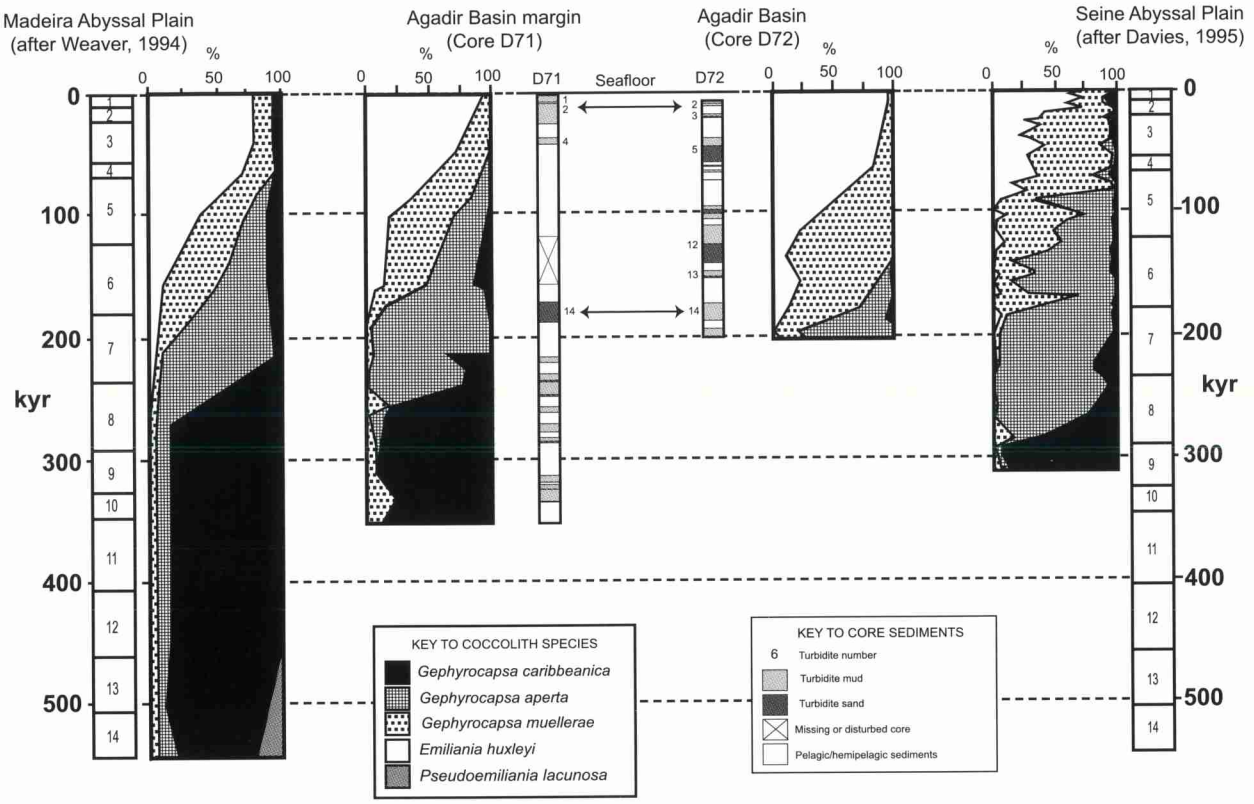

Fig. 7. Pelagic stratigraphy based upon coccolith ratios for cores D71 and D72 in the Agadir Basin, compared with those documented previously on the Madeira Abyssal Plain (Weaver, 1994) and the Seine Abyssal Plain (Davies, 1995). The oxygen isotope stratigraphy (after Martinson *et al.*, 1987) is included to provide dating control, and the coccolith ratio graphs and core logs are scaled to this. The positions of turbidites *AB1* to *AB14* are indicated in the two cores, relative to the pelagic stratigraphy. This confirms their positions as being at the oxygen isotope stage 1/2 and 6/7 boundaries, which are dated 12 ka and 190 ka respectively.

5 Relative position within the stratigraphic sequence. Certain intervals within cores have a very distinctive appearance, e.g. grey turbidite overlying brown clay overlying olive-grey turbidite overlying a pale ooze. Where these intervals are repeated between cores, they provide important markers that help to confirm correlations made using other techniques.

It is important to recognize that this combination of five different techniques ensures that the correlation is extremely accurate. All techniques were cross-referenced against each other, and the correlation is shown to be in agreement using all techniques, as illustrated in Figs 5–7. The correlation has allowed a numbering system for individual turbidites to be established. Each turbidite is numbered on the basis of its position within the sedimentary sequence, with *AB1* being at the top and *AB15* at the base. The key characteristics of the Agadir Basin turbidites are displayed in Table 2, and the correlated basin-fill sequence is shown in Fig. 8. In the following description, turbidites are divided into four groups, based on their mineralogy, colour and magnetic susceptibility.

Group 1 (Morocco Shelf source)

The muddy tops of turbidites *AB1*, *AB3*, *AB5*, *AB6*, *AB9*, *AB10*, *AB11*, *AB12*, *AB13* and *AB15* are all olive-green to olive-grey in colour (Table 2), indicating high organic matter contents (de Lange *et al.*, 1987). The sand fraction mineralogy is dominated by quartz, glauconite, clastic lithics, pyrite, mica, iron oxide and dolomite (Figs 4 and 5). Biogenic constituents include pelagic and benthic foraminifera, siliceous sponge spicules, phosphatic fish teeth and vertebrae, echinoid spines and shallow-water bivalves. Fragments of lignitic wood have also been discovered (Fig. 4). Magnetic susceptibility values are low, in the range 0–50 SI units (Fig. 6). In addition, a number of turbidites seen in core D73 below *AB15* are also believed to be group 1 turbidites (Fig. 8). They are

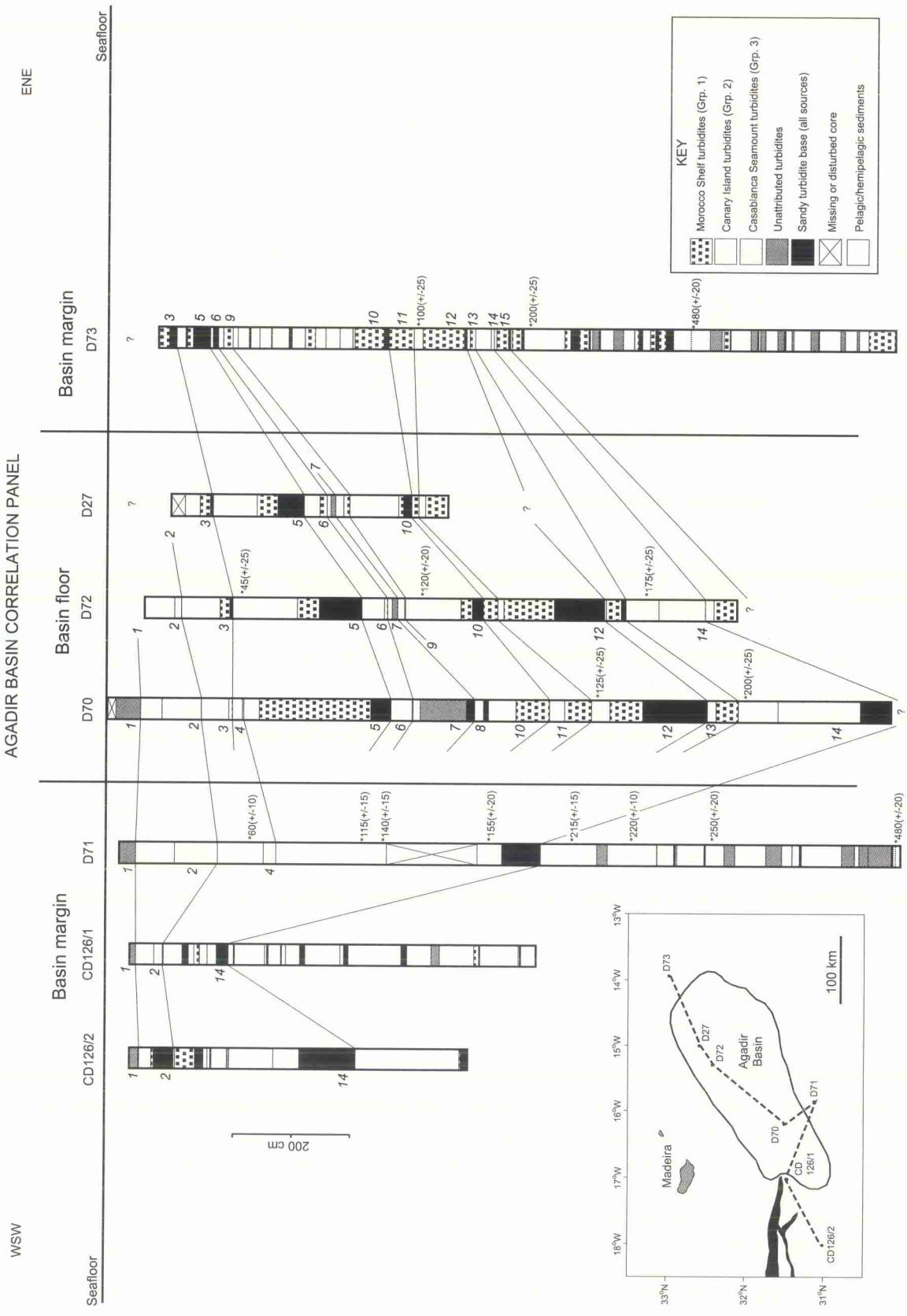

Fig. 8. Core correlation panel for the Agadir Basin sequence showing the turbidite fill. Numbers shown in italics indicate the turbidite number within the sequence. Dates marked with an asterisk (*) indicate age (in ka) of pelagic sediments based on coccolith dating and comparison with the oxygen isotope stratigraphy (after Martinson *et al.*, 1987). Sand bodies are highlighted with black shading. Core locations and the correlation line are shown on the inset map.

all < 40 cm thick and display similar characteristics to the group 1 turbidites seen higher in the sequence; however, they are not included in the correlated sequence as they are not penetrated by any of the other cores.

Group 1 turbidites contain a number of indicators suggesting they are sourced from the shallow waters of the continental shelf and upper slope. Glauconite is abundant and is thought to form on the open continental shelf and upper slope at water depths of 15–500 m (Rothwell, 1989). In addition, the presence of clastic lithic fragments, shallow-water bivalves and lignitic wood point to a nearshore origin. Further evidence of a shallow-water source for group 1 turbidites is shown by the presence of certain species of benthic foraminifera. These occur as pale green glauconitized casts and include *Elphidium crispum* and *Amphistigina* sp., both of which are found at the present day in water depths of < 150 m. However, it is interesting to note that Summerhayes *et al.* (1976) suggested that the majority of glauconite and pyrite present on the Morocco Shelf has been derived from Miocene strata outcropping on the outer shelf. Therefore, it seems possible that not all the shallow-water indicators are representative of modern shelf conditions. Despite this, they still provide good evidence for a Morocco Shelf source for group 1 turbidites, even if they are derived from outcropping strata on the outer shelf. None of the group 1 turbidites contain more than 1% aeolian quartz grains. This also indicates that they were probably sourced from the continental shelf north of the Canary Islands, as turbidites derived from the shelf south of the islands are generally dominated by aeolian quartz (Summerhayes *et al.*, 1976).

The mineral composition of group 1 turbidites shows some interesting trends. For example, the percentage of quartz always increases as grain size decreases. About 90% of the very fine sand fraction is made up of quartz, as opposed to 30–80% in the fine sand fraction (Fig. 5). This is because of the higher durability of quartz compared with other minerals and its resistance to chemical breakdown in the marine environment (Rothwell, 1989). However, for a given grain size, the proportion of minerals in individual Morocco Shelf turbidites generally remains similar throughout the basin. The exception is turbidite *AB5*, in which the proportion of pyrite shows a marked distal reduction. This is attributed to the high density of this mineral because, as the turbidity current loses energy distally, pyrite drops out of suspension more rapidly than other minerals of a similar size.

Turbidite *AB3* is slightly different from other Morocco Shelf turbidites in that it contains a high proportion of iron oxide flakes (Fig. 5). These are probably limonite (hydrated iron oxide), which is commonly associated with submarine volcanic provinces (Rothwell, 1989). However, the fine sand fraction (< 180 μm) also contains abundant quartz, glauconite and dolomite suggesting a Morocco Shelf source. This turbidite is therefore interpreted as being sourced from the flanks of one of the seamounts bordering the Agadir Canyon (Figs 1 and 2). The shelf-derived components (e.g. glauconite) present in the fine sand fraction may have been transported onto the slopes adjacent to the Agadir Canyon by some of the very large-volume turbidity currents that crossed this area before the deposition of *AB3*, such as turbidite *AB5*. Turbidite *AB3* is therefore sourced in deeper water beyond the shelf-break but, for the purposes of this study, it has been included within the Morocco Shelf group of turbidites.

Group 2 (Canary Island source)

Turbidites *AB2*, *AB4*, *AB8* and *AB14* generally display a distinctive sand fraction mineralogy, with volcanic glass and volcanic lithics being dominant (Figs 4 and 5). The volcanic glass occurs in a variety of morphologies, including pipe vesicles and bubble wall shards. Small amounts of pyrite and mica may also be present, and biogenic constituents include foraminifera and siliceous sponge spicules. Quartz contents are generally < 2%. Magnetic susceptibility values are typically very high, in the range 40–290 SI units (Fig. 6). The mud fraction of group 2 turbidites is grey or grey-brown in colour, with dark grey or black silt/sand bases (Table 2). Three additional volcaniclastic turbidites are present in core D71 below *AB14* (Fig. 8). These are not included in the correlated sequence as they are not penetrated by any other cores. All are < 40 cm thick and display similar characteristics to the other volcanic turbidites higher in the sequence.

Group 2 turbidites are interpreted as being derived from the submarine slopes of the volcanic Canary Islands, as they contain no shallow-water indicators, e.g. glauconite, and are dominated by volcanic glass and volcanic lithic fragments (Figs 4 and 5).

Group 3 (Casablanca Seamount source)

Five turbidites in the top 3 m of core D73 (Fig. 8) are not present in any other cores and are therefore very local in extent. They are all < 30 cm thick, with thin (< 4 cm) foraminifera sand bases and orange/red-brown muddy tops. Additional biogenic constituents include siliceous sponge spicules, echinoid spines and fish teeth. Magnetic susceptibilities are in the range 10–30 SI units, and there are no volcanic components in these turbidites.

Group 3 turbidites are interpreted to have been derived from the flanks of the Casablanca Seamount, which reaches 650 m below sea level, some 3400 m above the basin floor (CS on Fig. 1). The seamount flanks are draped by pelagic/hemipelagic sediments, which explains the dominance of biogenic material and the lack of mineral grains in the medium–coarse sand fraction of group 3 turbidites. However, the fine sand fraction often contains shelf-derived sediments similar to those seen in the Morocco Shelf turbidites. These sediments were probably transported onto the lower flanks of the seamount by earlier, large-scale turbidity currents. A Morocco Shelf source for these turbidites can be eliminated because of their localized distribution near to the base of the seamount. They are thus probably linked to small-scale failures on the seamount flanks, which would explain their small volume and restricted distribution.

Other sources (unattributed turbidites)

There are a number of turbidites within the Agadir Basin sequence that cannot be linked to a specific source area, and these are termed unattributed turbidites. An example is turbidite *AB7*. The sandy base of this turbidite is dominated by quartz, irregular pyrite and volcanic glass, and contains none of the shallow-water indicators (e.g. glauconite, clastic lithics) that would suggest a Morocco Shelf source. However, the mud fraction is olive-green in colour and is organic rich, which does indicate a source area on the north-west African margin (Pearce & Jarvis, 1992). In addition, unlike the Morocco Shelf turbidites, it is absent or very thin in the eastern Agadir Basin and the SAP. Turbidite *AB7* is tentatively interpreted as being derived from the submarine slopes of the eastern Canary Islands, although more core data from the adjacent margin are required to confirm this.

CORRELATION OF THE AGADIR BASIN SEQUENCE WITH THE MAP AND SAP SEQUENCES

Now that the turbidite sequence on the Agadir Basin has been successfully correlated, the next stage is to tie this sequence into those on the MAP and SAP. The turbidite depositional histories of these abyssal plains have already been well documented (Weaver & Kuijpers, 1983; Rothwell *et al.*, 1992; Weaver *et al.*, 1992; Weaver, 1994; Davies, 1995; Davies *et al.*, 1997), and summary correlation panels for the two sequences are shown in Figs 9 and 10. Using the combination of techniques described above (sand fraction composition, magnetic susceptibility, turbidite colour, micropalaeontological dating and relative stratigraphic position), a number of turbidites in the Agadir Basin sequence can be correlated with turbidites in the MAP and SAP sequences. Again, it should be stressed that a combination of techniques has been used to ensure the accuracy of the correlation. As discussed later, not all techniques can be applied across the whole system. For example, sand fraction mineralogy is not applicable to correlation of the Agadir Basin and MAP turbidites, as the sandy fractions of these turbidity currents are shown to evolve during their passage through the Madeira Distributary Channel System. However, the results obtained indicate that the muddy fractions of these flows do not mix during the passage between basins and, therefore, the correlation based upon other techniques, e.g. coccolith analyses (Fig. 11) and turbidite mud colour, should remain unaffected. This conclusion is further substantiated by the work of Weaver (1994), which indicated that the total amount of eroded material (including both sand and mud fractions) incorporated into turbidity currents during their passage from the Morocco Shelf/Canary Islands to the MAP was < 15%.

The Agadir Basin turbidite sequence has been tied into core D13 on the MAP and core D74 on the SAP, and the results of the correlation are displayed in Fig. 12 and Table 3. Turbidites *AB5*, *AB10*, *AB12* and *AB14* are the only turbidites to occur in all three basins. In the following discussion, the correlated turbidites will occasionally have their abyssal plain correlations displayed in parentheses. Therefore, turbidite *AB5* will be displayed as *AB5*(*Md/Se*), indicating that turbidite *AB5* in the Agadir Basin has been correlated with turbidite *Md* on the MAP and turbidite *Se* on the SAP.

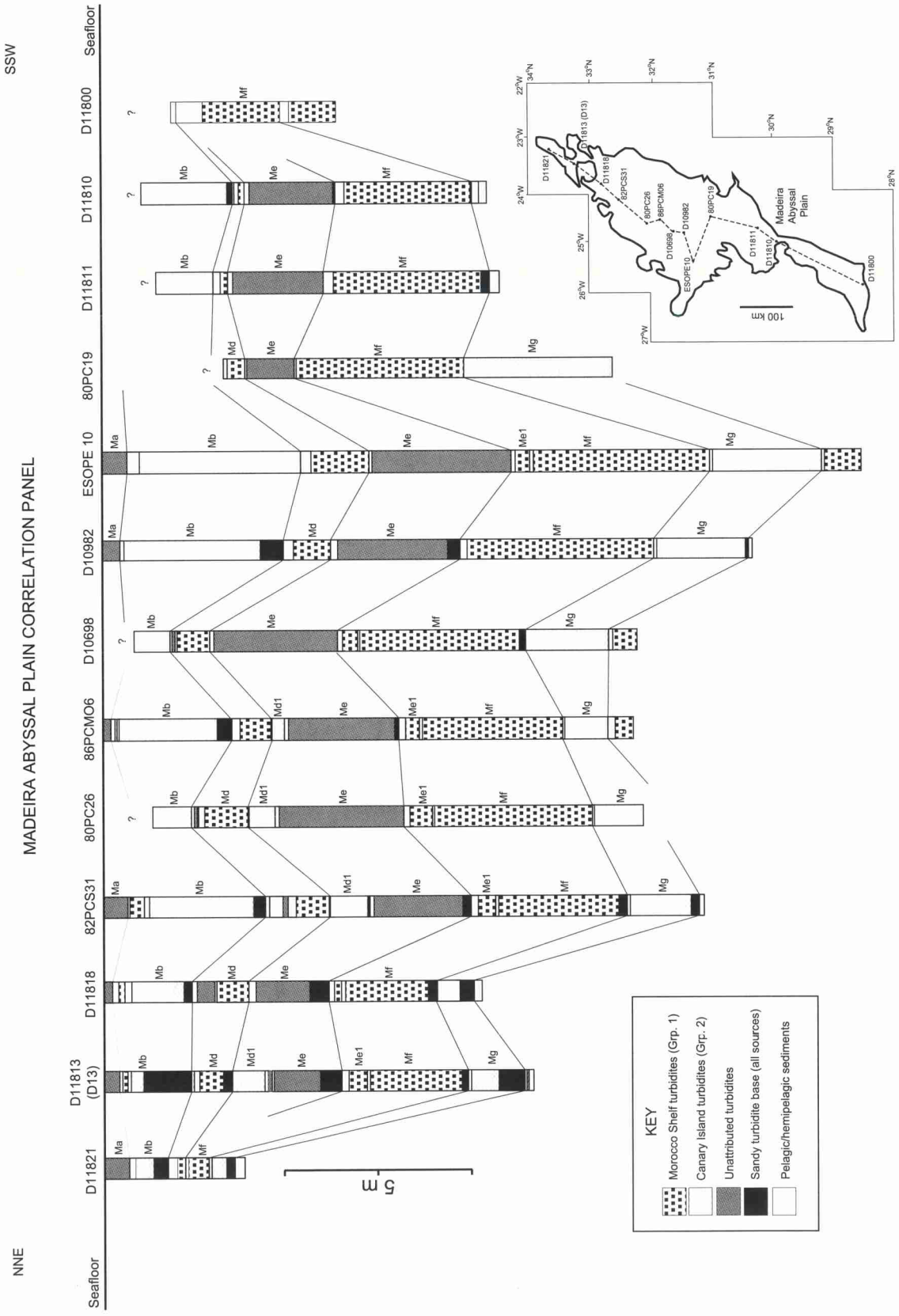

Fig. 9. Core correlation panel for the Madeira Abyssal Plain sequence showing the turbidite fill (modified from Weaver *et al.*, 1992). Letters shown indicate the turbidite letter within the sequence. Sand bodies are highlighted with black shading. Core locations and the correlation line are shown on the inset map.

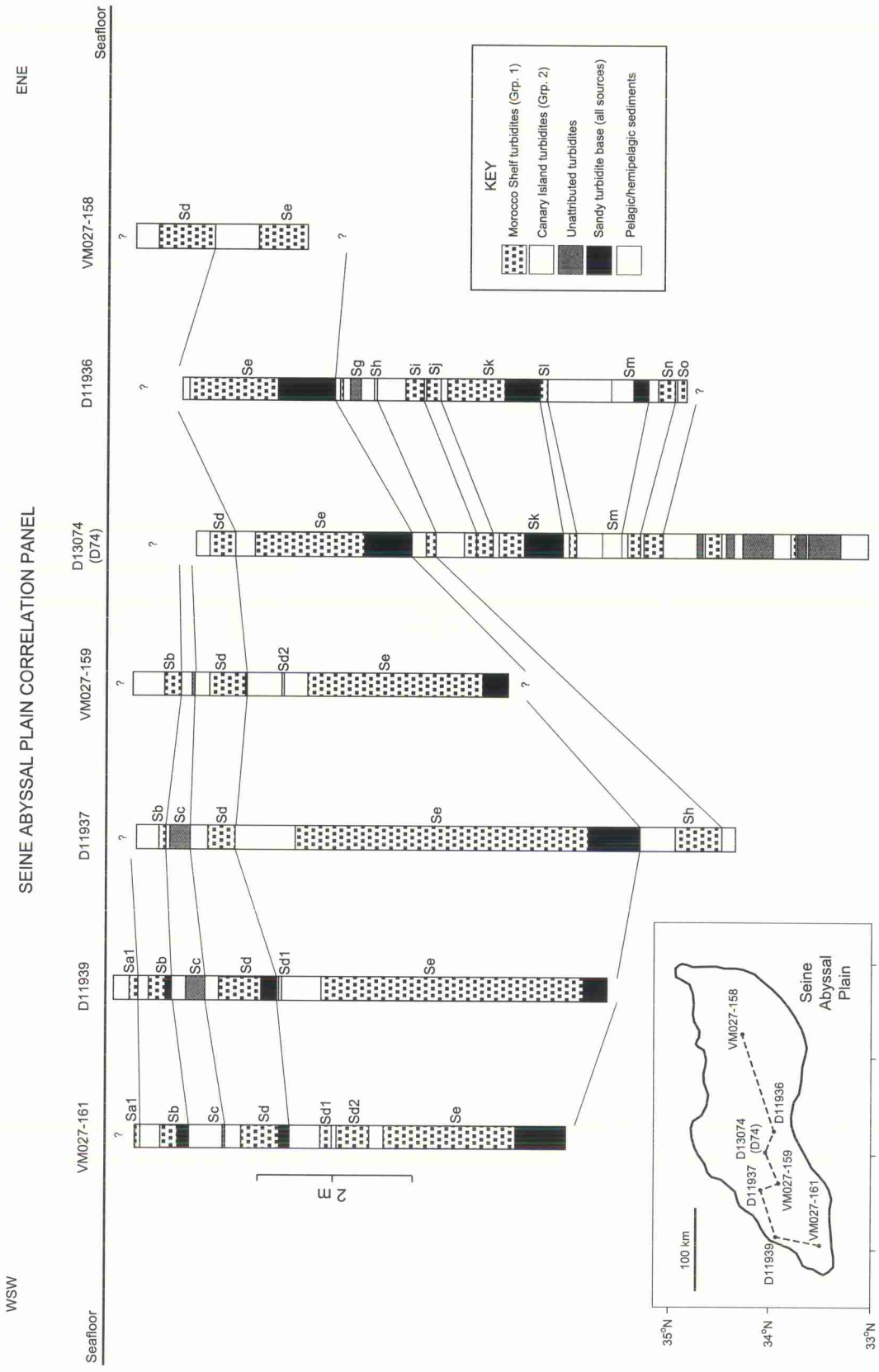

Fig. 10. Core correlation panel for the Seine Abyssal Plain sequence showing the turbidite fill (modified from Davies, 1995). Letters shown indicate the turbidite letter within the sequence. Sand bodies are highlighted with black shading. Core locations and the correlation line are shown on the inset map.

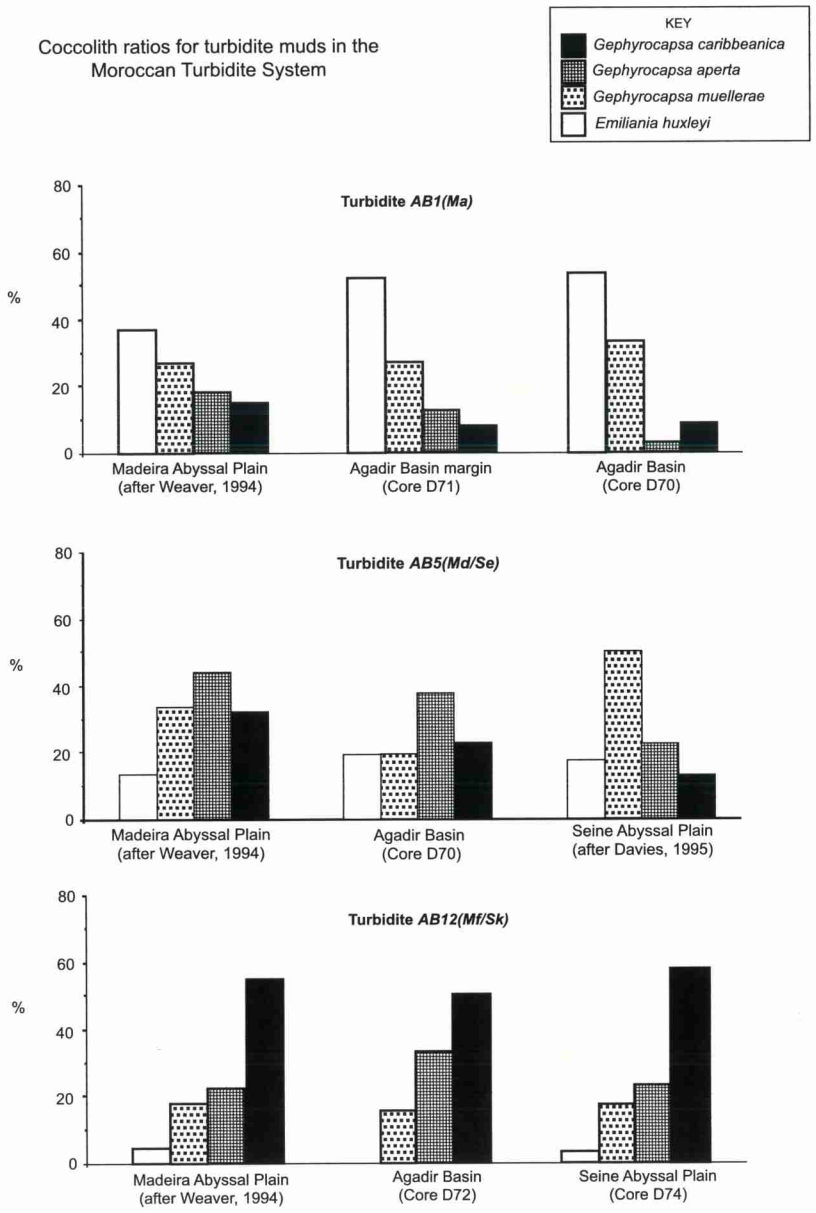

Fig. 11. Diagram illustrating the coccolith ratios in the mud fraction of three individual turbidites across the MTS. Note how the coccolith ratios are similar for *AB5(Md/Se)* and *AB12(Mf/Sk)* in all three basins, indicating that the muddy suspended load of these turbidity currents has not been involved in extensive sea-floor erosion.

TURBIDITE VOLUMES

The estimated volumes of each turbidite have been calculated on the basis of their thickness and areal distribution in the Agadir Basin, SAP and MAP (Table 3). It should be noted that these values are only estimates, as it is not possible to quantify the precise volume of individual turbidites on the slope and rise because of lack of core control. In addition, the core control within basins is not evenly distributed and, therefore, volume calculations based upon turbidite thickness values in cores will have an inherent error. The possible error has been calculated for several turbidites as $\approx 20\%$. Table 3 displays the maximum thickness and estimated volume of each turbidite in the three basins. In addition, the total volume of each turbidite is presented, as well as the turbidite age (based upon oxygen isotope stage boundaries). The volume data show an interesting pattern, with a wide range of total volumes. The largest turbidite is *AB12(Mf/Sk)*, which, with a total volume of 200–300 km^3, is considerably larger than any of the other turbidites. Four additional large-volume turbidites [*AB2(Mb)*, *AB5(Md/Se)*, *AB7(Me)* and *AB14(Mg/Sm)*] have total volumes >100 km^3, with all the other turbidites being <35 km^3.

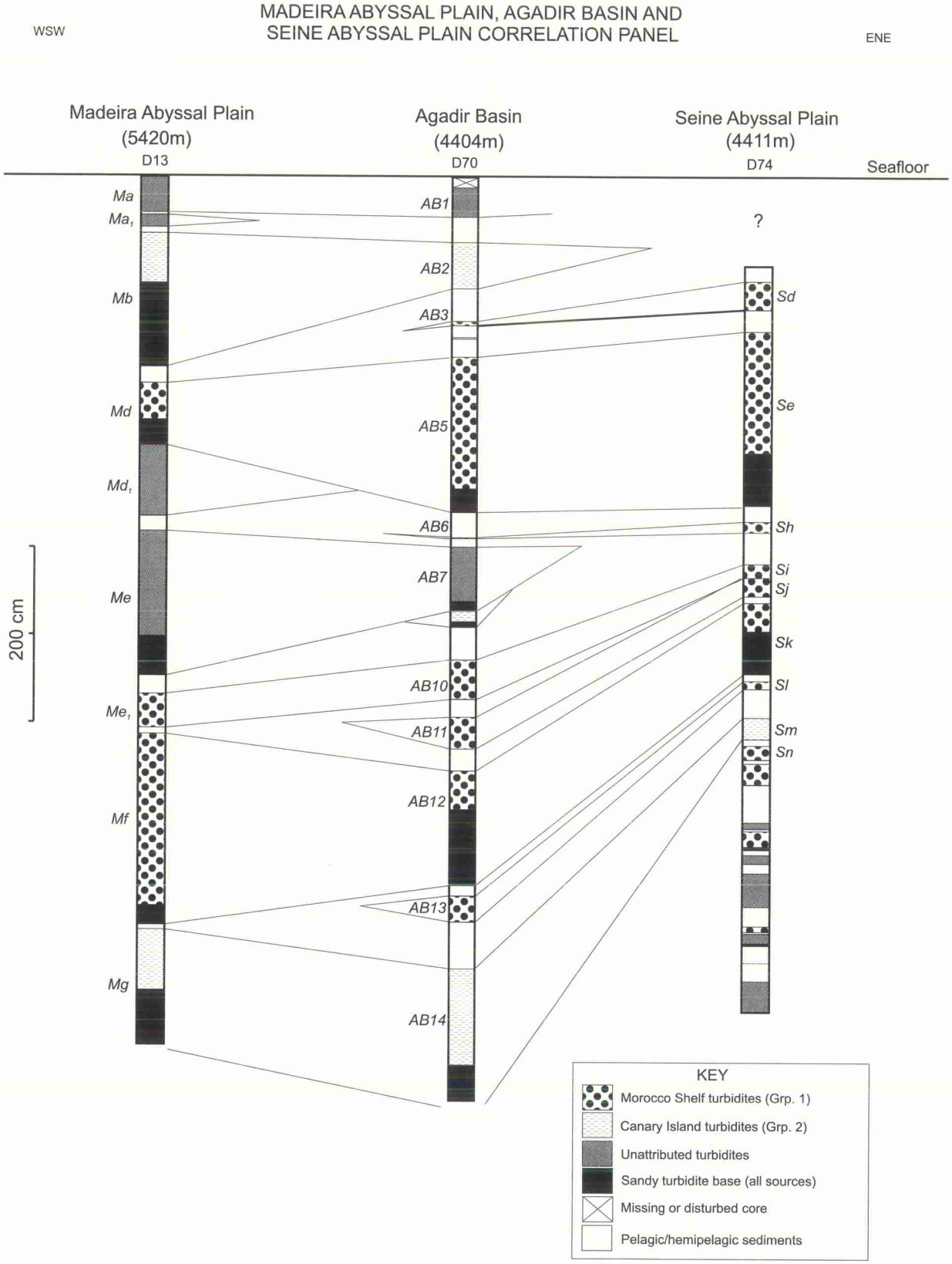

Fig. 12. Core correlation panel for the Madeira Abyssal Plain, Agadir Basin and Seine Abyssal Plain. Numbers shown in italics indicate the turbidite number within the Agadir Basin sequence (Fig. 8), whereas letters shown in italics indicate the turbidite letter within the MAP sequence (Weaver & Kuijpers, 1983) and the SAP sequence (Davies *et al.*, 1997). Sand bodies are highlighted with black shading. Core locations are shown in Fig. 1b.

Table 3. Correlation of turbidites in the MAP (Rothwell *et al.*, 1992; Weaver *et al.*, 1992), Agadir Basin (this study) and SAP (Davies, 1995) sequences, with estimated volume and maximum thickness shown for each turbidite.
The position of each turbidite within the oxygen isotope stratigraphy is shown, together with the dating control based upon this stratigraphy (after Martinson *et al.*, 1987). The five large-volume (> 100 km^3) turbidites are highlighted by grey shading.

Madeira AP (68,000 km^2)			Agadir Basin (~38,000 km^2)			Seine AP (37,500km^2)					
Letter	*Max thickness (cm)*	*Vol. (km3)*	*No.*	*Max thickness (cm)*	*Vol. (km3)*	*Letter*	*Max thickness (cm)*	*Vol. (km3)*	*Total volume (km3)*	Position in oxygen isotope stratigraphy	*Age (ka)**
a	120	?	1	34	?				?	Near top of stage 1	<1**
b	500	100-150	2	54	5-10				105-160	At stage 1/2 boundary	12
			3	24	3-5	d	75	9-13	12-18	At stage 2/3 boundary	24
			4	17	1-3				1-3	Within stage 3	24-59
d	150	25-35	5	177	30-45	e	445	48-71	100-150	At stage 3/4 boundary	59
			6	10	1-3	h	60	3-5	4-8	Within stage 4	59-71
e	300	90-130	7	75	11-17				100-150	At stage 4/5 boundary	74
			8	18	2-4				2-4	Within stage 5	74-130
			9	12	<1				<1	Within stage 5	74-130
e_1	60	6-10	10	46	10-16	i	35	6-8	22-34	Within stage 5	74-130
			11	34	7-11	j	20	5-7	12-18	Within stage 5	74-130
f	500	150-230	12	135	30-45	k	115	27-31	200-300	At stage 5/6 boundary	130
			13	30	6-10	l	10	2-4	8-14	Within stage 6	130-190
g	250	55-85	14	151+	>29	m	45	10-16	>95	At stage 6/7 boundary	190
			15	32+	>12	n	20	5-7	>17	Within stage 7	190-244

* after Martinson *et al.* (1987)

** after Thomson & Weaver (1994)

DISCUSSION

Basin connectivity in the MTS

Detailed correlation of individual turbidites has revealed that large-volume turbidites (> 100 km^3) derived from the Morocco Shelf and the Canary Islands are present in three different depositional basins. Turbidites *AB5*(*Md/Se*) and *AB12*(*Mf/Sk*) are both sourced from the Morocco Shelf and are present in the SAP, the Agadir Basin and the MAP basin-fill sequences (Fig. 12). The turbidity currents that produced these deposits transported material from the Morocco Shelf through the Agadir Canyon (Figs 1 and 2). These flows must have divided at the canyon mouth as they became unconfined, and one part flowed northwards and entered the SAP via an intrabasinal sill (Davies *et al.*, 1997). The remainder of the flow travelled westwards through the Agadir Basin and then passed through the northern section of the Madeira Distributary Channel System (MCDS) before terminating on the MAP (Figs 1 and 2). Turbidite *AB14*(*Mg/Sm*) is sourced from the Canary Islands and is also present in all three basins (Fig. 12). The major part of this turbidity current flowed north-west and passed through the southern section of the MDCS before terminating on the MAP. The remainder of the flow would have travelled northwards around the western slopes of the Selvage Islands before entering the Agadir Basin from the west (Figs 1 and 2). This flow then travelled north-eastwards across the gentle gradients of the basin floor, and a small amount of the muddy suspended load passed over the intrabasinal sill (> 100 m above the basin floor) into the SAP.

The analysis of turbidity current pathways discussed above has been made possible by good-quality core control in all three basins and highlights the unique nature of this turbidite system. This is the first documented example of a turbidite system in which individual flows can deposit sediments in three different depositional basins across a distance of >1200 km. Other studies have also described turbidity currents passing from one basin to another (e.g. Heezen *et al.*, 1959; Laughton, 1960), and it has been suggested that turbidity currents can be rejuvenated by the increase in gradient and lateral constriction as they pass through intrabasinal passages (Laughton, 1960). However, these studies generally describe systems in which the passage between basins involves flow constriction or channellization, which is not the case in some parts of the MTS, e.g. between the Agadir Basin and the SAP (Figs 1 and 2).

Turbidite mineralogy: implications for turbidity current flow processes

In a study of the MDCS, Masson (1994) commented on the presence of volcanic components in turbidites derived from the Moroccan margin and suggested that some Morocco Shelf turbidity currents incorporate volcanic material picked up from the MDCS on their passage downslope. The volcanic material had been deposited within the MDCS by earlier volcaniclastic turbidity currents, indicating that both erosion and deposition can occur within this channel system. This study reveals that a number of turbidites correlated between the Agadir Basin and the MAP show significant lateral variation in mineralogy, and this is also interpreted as evidence for channel floor erosion.

Turbidites *AB5*(*Md*) and *AB12*(*Mf*) in the Agadir Basin sequence can be classified by source area on the basis of their sand fraction mineralogy (Fig. 5). Throughout the basin, the sandy bases of these turbidites show a distinctive mineralogy from the Morocco Shelf, with a total absence of any volcanic components. However, when the same turbidites are sampled on the MAP, after having passed through the MDCS, the sand composition is generally very different from that seen upslope in the Agadir Basin (note that the correlation between the Agadir Basin and the MAP can still be completed with confidence using other techniques, e.g. micropalaeontological dating). All the turbidite sands in the MAP are dominated by pelagic foraminifera, sponge spicules, biotite and volcanic glass, with smaller amounts of quartz, glauconite and volcanic lithics. The dominance of foraminifera, spicules, biotite and volcanic glass over the other grain types can be explained in part by their lower effective density that affects transport potential, i.e. for a given grain size, these components will be transported a greater distance. However, this does not explain why turbidites containing no volcanic material in the Agadir Basin are found to contain significant numbers of volcanic grains on the MAP. This is interpreted as a result of sea-floor erosion and flow evolution within the MDCS. When flows sourced from the Morocco Shelf pass through this channel system, they erode some of the previously deposited volcaniclastic turbidite sands, which explains why many turbidites on

the MAP have a mixed Morocco Shelf/Canary Island mineral assemblage.

Masson (1994) also concluded that separation of different parts of the flow probably occurs within the channel system, whereby the sandy bedload of the turbidites is transported within the confines of the channel, and the finer grained suspended load is unconfined as it crosses the continental rise. The sandy turbidite bedload forms two distinct sandy lobes at the termination of the northern and southern sections of the MDCS (Wynn *et al.*, 2000), confirming that the passage of turbidite sands has been channellized. The finding that the fine-grained suspended load is unconfined is also reinforced by geochemical analysis of the turbidite muds on the MAP, which shows that individual turbidites have retained their signature of source composition, i.e. as sourced on the Canary Islands or Morocco Shelf (de Lange *et al.*, 1987). In addition, the unique coccolith ratios in each turbidite remain essentially the same between the Agadir Basin and the MAP (Weaver, 1994). Three examples of this are shown in Fig. 11, where, for example, turbidite *Mf* from the MAP has been correlated with turbidite *AB12* from the Agadir Basin and turbidite *Sk* from the SAP. In all three cores, the coccolith ratios in the turbidite mud are very similar; the species *Gephyrocapsa caribbeanica* has between 50% and 60% of the totals, *Gephyrocapsa aperta* has 25–35% and *Gephyrocapsa muellerae* has 10–20%. These results indicate that the mud fraction of individual turbidites on the MAP has not evolved significantly during transport between the Agadir Basin and the MAP and, therefore, the muddy part of the flow is unlikely to have interacted with previously deposited sea-floor sediments on the passage downslope. This is in contrast to the findings discussed above relating to the turbidite sands, whereby the sand fraction of turbidity currents is channellized as it passes through the MDCS and undergoes flow evolution resulting from channel floor erosion/deposition.

Interpretation of turbidite sedimentary structures

A wide variety of sedimentary structures are present in the Agadir Basin turbidites, although only *AB5* and *AB12* display a complete Bouma sequence (Bouma, 1962) from T_a to T_e. Many turbidites show a progressive base cut-out of the lower Bouma divisions (T_a–T_c) in the distal basin, whereas the thinner turbidites are often composed entirely of T_d and T_e silts and muds. The Bouma T_c division of convolute-laminated and cross-laminated silts is commonly developed, although undeformed cross-laminae are rare, as noted in turbidites on the MAP by Rothwell *et al.* (1992). Two of the largest turbidites in the Agadir Basin [*AB5*(*Md*) and *AB14*(*Mg*)] show a series of sedimentary structures that allows interpretation of their formative flow processes. Both these turbidites often have a complex coarse basal facies (T_a–T_b) that can be correlated across the basin.

Turbidite *AB5* (Fig. 4) has a thin, erosive, sandy base (T_a) overlain by laminated coarse to fine sands (T_b). The T_c division shows variable development; in the eastern basin, it consists of convolute laminae and cross-laminae, occasionally containing small mud clasts. In the western basin, it consists of fine sand/muddy silt laminae that are often contorted and lenticular and contain irregular silty blebs. The convolute laminae are interpreted as being formed by shear deformation, in which deposition of the coarse-grained bedload results in the deformation of underlying unconsolidated laminated and cross-laminated silts (Rothwell *et al.*, 1992). The mud clasts and silty blebs are also associated with disturbance and erosion of ripple and convolute laminae by bedload shear (Stow & Shanmugam, 1980). The top of turbidite *AB5* comprises T_d division silt-mud laminae and T_e division muds. The T_e division can be further subdivided according to the classification scheme of Piper (1978). In turbidite *AB5*, E_1 laminated muds are overlain by E_2 and E_3 structureless bioturbated muds.

Turbidite *AB14* (Fig. 4) shows a basal sequence of multiple, often coarsening-upward packages, 1–7 cm in thickness, which are composed of silt-mud laminae. Overall, this laminated unit grades from coarse silt and silty mud at the base to fine silt and mud at the top. This basal sequence is interpreted as being (1) the result of deposition from a surge-type turbidity current with fluctuating flow velocities (Lowe, 1982; Rothwell *et al.*, 1992; Kneller, 1995); (2) the result of flow reflection within the basin (Rothwell *et al.*, 1992); or (3) a product of the trigger mechanism, which may have been a retrogressive failure with several phases of movement (e.g. Gardner *et al.*, 1999). Towards the top of this laminated unit, very regular alternations between slightly lenticular laminae and cross-laminae may represent the T_c division. The top of the turbidite consists of T_e division muds, with E_1 laminated muds overlain by a thick

sequence of E_2 and E_3 structureless bioturbated muds (Piper, 1978).

Turbidite depositional architecture of the Agadir Basin

The complex topography of the north-west African margin is responsible for creating an unusual turbidite system, with multiple, widely spaced source areas and a depositional basin containing a complex turbidite fill. The turbidite architecture of the MAP and the SAP has already been covered in detail (Rothwell *et al.*, 1992; Davies, 1995; Davies *et al.*, 1997; Wynn *et al.*, 2000), and several types of turbidite sand body can be recognized. For example, on the MAP, sands are concentrated around channel terminations at the break-of-slope and form distinct depositional lobes (Wynn *et al.*, 2000). On the SAP, sands onlap the lower rise forming a linear wedge (Davies, 1995). In both cases, overlying turbidite muds tend to be ponded deposits that infill topographic lows on the plain. Linear, sand-rich turbidite deposits are present in the distal Agadir Canyon and the MDCS (e.g. Masson, 1994) but, owing to lack of core control, these are poorly documented. However, the total volume of sand present within these channels is likely to be insignificant compared with the large volumes present in the basin-fill sequences.

This discussion now concentrates on the turbidite depositional architecture of the Agadir Basin, which contains turbidites derived from two main source areas: the Morocco Shelf and the volcanic Canary Islands. Turbidites from these different source areas show different patterns of bed thickness and sand/mud ratio, but even turbidites from the same source area have a highly variable distribution. For example, three turbidites derived from the Morocco Shelf all have a different architecture. Turbidite *AB3* is thickest in the eastern basin fill (proximal to the Morocco Shelf) and thins distally (Fig. 13). The sand/mud ratio is about 35:65 in the eastern basin, but decreases to 20:80 in the central basin and to 0:100 in the western basin. The opposite trend is shown by turbidite *AB5*, which is thinnest in the eastern basin and thickens distally (Fig. 13). The sand/mud ratio decreases from 75:25 in the eastern basin to 60:40 in the central basin and 10:90 in the western basin. Turbidite *AB12* is different again, showing a fairly uniform thickness across the whole basin (Fig. 13). However, the sand/mud ratio is only 10:90 in the eastern basin, but increases to 40:60 in the central basin and to 65:35 in the western basin.

The question therefore arises as to why turbidites derived from a single source area have such a variable architecture? The answer is probably related to turbidite volume, as the three turbidites described above have estimated total volumes of < 35 km^3, 100–150 km^3 and 200–300 km^3 respectively (Table 3). This wide range of volumes suggests that the original turbidity currents would have had different potential energy as they exited the Agadir Canyon and passed through the Agadir Basin, leading to variations in depositional architecture.

1 Turbidite *AB3* (< 35 km^3) was probably wholly contained within the Agadir Canyon and, on exiting the canyon, would have undergone rapid lateral flow expansion as it spread across the basin floor. The resulting loss of energy would lead to sand deposition close to the canyon mouth and gradual dissipation of flow energy as it continued south-eastwards. Turbidite *AB3* was therefore only deposited within the Agadir Basin and is absent from the MAP sequence further west (Fig. 13).

2 Turbidite *AB5* (100–150 km^3) is too large to have been confined within the Agadir Canyon, and most of the fine-grained suspended load was probably unconfined as it crossed the slope and rise before entering the basin. At the canyon mouth, an increase in turbulence, possibly linked to a hydraulic jump, led to intense sea-floor erosion and the development of large-scale scours (up to 10 m deep × 0·5 km wide × 1 km long) within the channel termination zone (Fig. 14; Wynn *et al.*, 2002). The erosional scours cannot be linked directly to the turbidite deposits of *AB5* (as observed in the Agadir Basin cores), but have undoubtedly been generated by high-energy flows, and turbidite *AB5* is the most recent large flow to have passed through the scour zone. Therefore, it seems reasonable to assume that the scours were generated, or maintained, by the *AB5* turbidity current. Core data indicate that almost all the fine-grained suspended load was transported westwards to the distal Agadir Basin before deposition. The sandy load was deposited beyond the channel termination zone in the proximal and central basin. Only a relatively small fraction of the turbidity current load bypassed the Agadir Basin before deposition on the MAP (Fig. 13).

3 Turbidite *AB12* (200–300 km^3) was deposited by the largest turbidity current to have crossed the Agadir Basin in the last 200 000 years.

This flow would have been similar in nature to that which deposited turbidite *AB5*. However, the larger volume and presumably higher energy of the flow that deposited turbidite *AB12* meant that much of the fine-grained suspended load was transported completely beyond the Agadir Basin, and was finally deposited some 500 km further west on the MAP. Therefore, although the sandy base of this turbidite on the MAP is of a similar thickness to turbidite *AB5*, the mud fraction is about five times thicker (Fig. 13). The flow energy within the Agadir Basin was also sufficiently high for the sandy load to be deposited at a constant thickness across the basin.

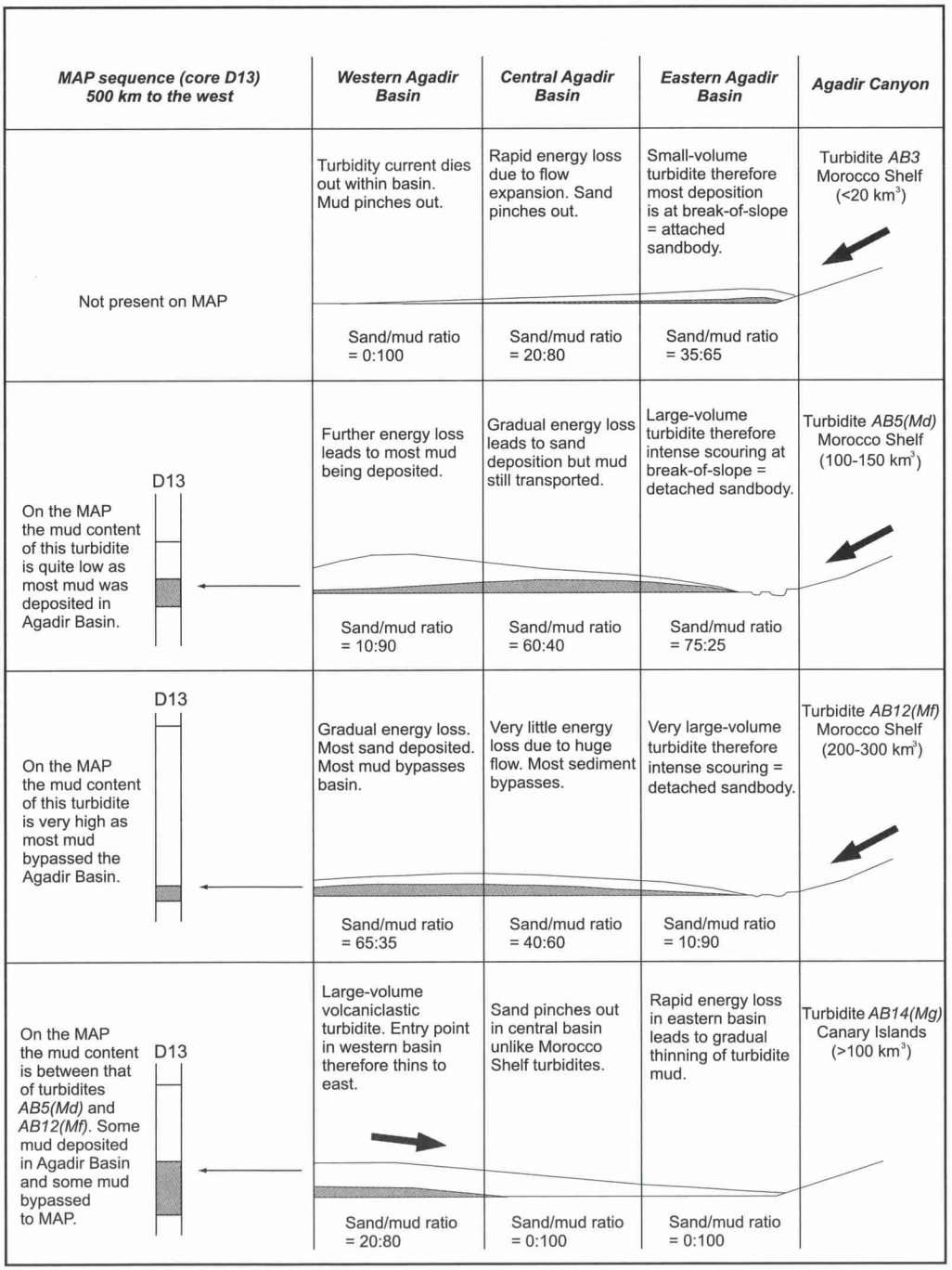

Fig. 13. Schematic diagram showing the depositional architecture of four different turbidites in the Agadir Basin, together with a comparison of their appearance in core D13 from the MAP. Note how the architecture of the three Morocco Shelf turbidites varies as a result of their different volumes. Black arrows indicate turbidity current flow direction. Diagram not to scale.

It is interesting to note that none of the Morocco Shelf turbidites discussed above is present in core D71, recovered from the lower rise at a height of 100 m above the basin floor (Fig. 1b). This indicates that none of these flows was >100 m in thickness as they crossed the central Agadir Basin, probably because of intense flow thinning as the flows expanded across the 100-km width of the Agadir Basin. However, several flows were sufficiently large to cross the broad intrabasinal sill separating the Agadir Basin from the SAP, which is about 40 m high at its lowest point. Core D73, recovered from near the high point of the sill, shows a highly condensed turbidite fill compared with that seen on the floor of the adjacent Agadir Basin and the SAP (Fig. 8). However, all the turbidites present on either side of the sill display sand continuity across this barrier, although the sandy bases are generally coarser and thinner and are capped by thin T_e division muds. This is partly caused by erosional processes, as many turbidite bases on the levee crest are eroded into underlying turbidite muds.

Although variations in turbidite volume appear to be one contributing factor to the complexity of the basin fill, the presence of multiple source areas is another significant factor. Turbidites derived from the Canary Islands are generally thickest in the western and central Agadir Basin and thin or pinch-out to the east (Fig. 13). This is in the opposite direction to most of the Morocco Shelf turbidites and results from the Canary Island turbidites having a south or south-west entry point into the basin, as opposed to the Morocco Shelf turbidites, which enter from the east and south-east. To summarize, the complex turbidite depositional architecture of the Agadir Basin is interpreted as a function of varying turbidity current volume and flow energy, combined with multiple source areas and input points into the basin.

Controls on the timing of turbidite deposition in the MTS

Previous studies of the turbidite sequence on the MAP have revealed that all the large (> 100 km^3)

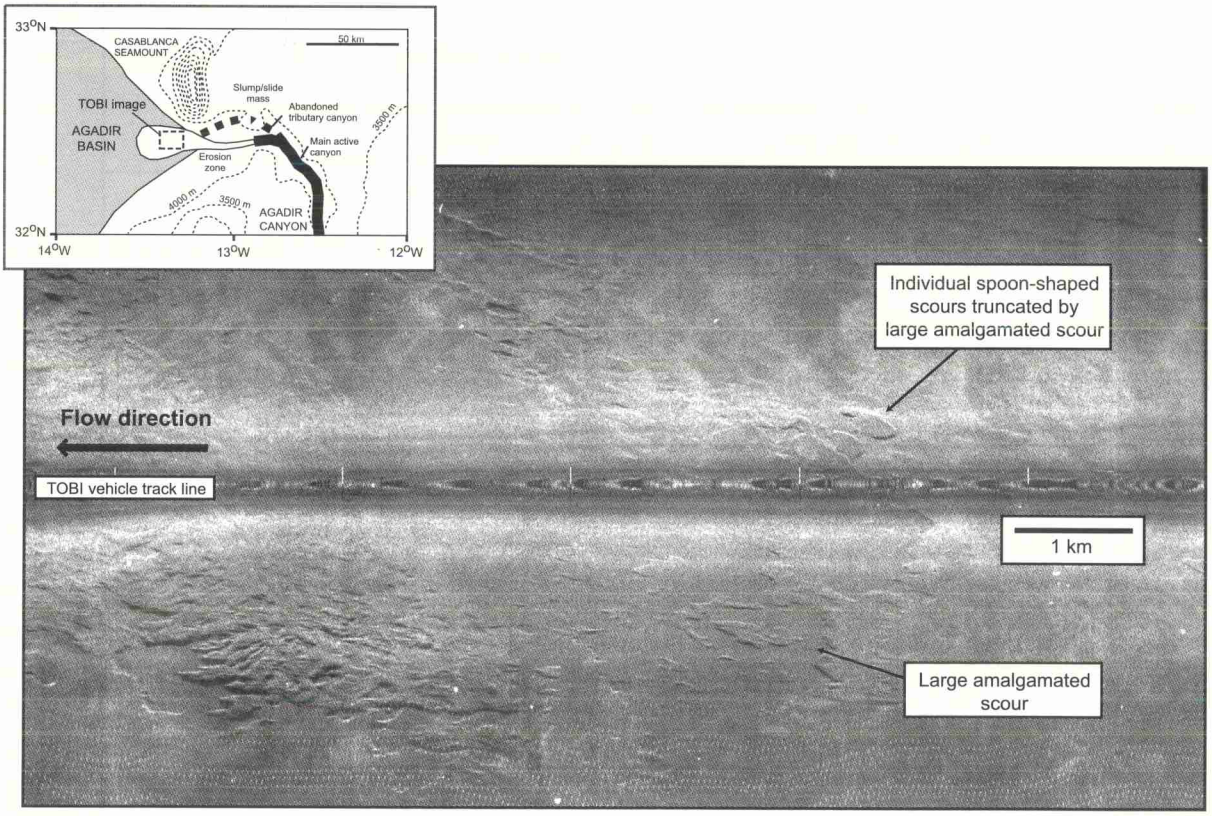

Fig. 14. TOBI high-resolution sidescan sonar image showing a large area of amalgamated scour and two individual spoon-shaped scours in an erosional zone beyond the mouth of the Agadir Canyon (modified from Wynn *et al.*, 2002). Illumination is outwards from the centre of the TOBI swath. Light tones, high backscatter; dark tones, low backscatter. The location of the TOBI image is shown on the inset map.

turbidites were deposited at oxygen isotope stage boundaries (Table 3) (Weaver & Kuijpers, 1983; Rothwell *et al.*, 1992; Weaver *et al.*, 1992). These boundaries represent periods of global climate change between glacial and interglacial conditions, when eustatic sea level was either rising or falling rapidly. In addition, Weaver & Kuijpers (1983) revealed that the three largest turbidites on the MAP (*AB2/Mb*, *AB7/Me*, and *AB12/Mf*) occurred during the largest fluctuations in sea level (based on the rate and relative amount of sea-level change), and also noted that nearly all the oxygen isotope stage boundaries are represented by a single large-volume turbidite on the MAP (Table 3). These findings contrast with many studies of submarine fans, which suggest that most turbidites are deposited during lowstands of sea level (e.g. Shanmugam & Moiola, 1981; Stow *et al.*, 1984). However, there is a growing body of literature showing that many turbidite systems remain, or become increasingly active, during sea-level rises or highstands (e.g. Zaragosi *et al.*, 2000).

In the last 750 000 years, turbidite frequency on the MAP has averaged one every 30 000 years (Weaver *et al.*, 1992). This compares with one turbidite every 16 000 years for the SAP (Davies *et al.*, 1997), indicating that turbidite frequency generally decreases with distance from the continental margin. In the Agadir Basin, turbidite frequency has averaged about one every 10 000 years, although there appears to be a major change in turbidite frequency at about 200 ka, which marks the start of the stage 6 glacial. Analysis of core D73 indicates that a total of 12 Morocco Shelf turbidites were deposited between 200 ka and the present day, but only about seven were deposited in the preceding 300 000 years (Fig. 8). This change was also noted by Rothwell *et al.* (1992) on the MAP, where there was a major switch in turbidite source areas at 200 ka. At this time, the dominant turbidite source area changed from the western Saharan margin to the Morocco Shelf and Canary Islands. Unfortunately, the reasons for this switch in turbidite frequency and source area are still poorly understood.

CONCLUSIONS

This study has revealed that turbidites in the MTS are derived from several source areas, including the Morocco Shelf, the volcanic Canary Islands and adjacent seamounts. Excellent core control has enabled the turbidite sequence for the last 200 000 years to be correlated between the Agadir Basin, the MAP and the SAP, providing new insights into turbidite depositional architecture across interconnected deep-water basins. Turbidite sand bodies on the MAP and SAP are generally concentrated at the break-of-slope and form radial lobes or longitudinal wedges aligned parallel-to-slope. However, within the Agadir Basin, extensive basin-wide sheet sands are developed. The thickness and lateral extent of these sheet sands is largely controlled by turbidite source area and volume. Turbidites derived from the Morocco Shelf all enter the Agadir Basin from the east or south-east, but show a highly variable architecture related to differences in volume. Very large-volume turbidity currents (200–300 km^3 of sediment) deposit most of their sand in the central and distal basin, but have enough energy to transport most of the mud fraction out of the basin and a further 500 km west before deposition on the MAP. They form large sand bodies that are separated from the Agadir Canyon mouth by a zone of erosional scours. Large-volume turbidity currents (100–150 km^3 of sediment) also deposit most of their sandy load in the central and distal basin, but lose sufficient energy to deposit most of the mud fraction in the distal basin. Small-volume turbidity currents (< 35 km^3 of sediment) are totally confined within the Agadir Basin and pinch out in the distal basin. They form small, thin sand bodies that are probably attached to the Agadir Canyon mouth. Turbidites derived from the Canary Islands enter the Agadir Basin from the south or south-west, and therefore show a different pattern of thickness and grain size from the Morocco Shelf turbidites. This paper illustrates that the turbiditic fill of some depositional basins can be highly complex in systems characterized by multiple sources and large variations in turbidity current volume.

ACKNOWLEDGEMENTS

We would first like to acknowledge the assistance of the ship staff during data collection on *RRS Discovery* cruise 225 and *RRS Charles Darwin* cruise 126. R.B.W. would like to acknowledge the provision of PhD funding from the University of Southampton and the SOC Challenger Division. D.A.V.S. acknowledges tenure of an RS Industry Fellowship and support from BP Amoco. Barry Marsh, Dipalee Patel and Ann Jurd (University of Southampton) are thanked for technical and

practical assistance. John Murray (University of Southampton) provided valuable information on formaminifera identification and distribution. The manuscript was greatly improved by the thorough reviews of Thierry Mulder and Hugh Sinclair, and the editing of Jim Best.

REFERENCES

Akil, M. and **Gayet, J.** (1988) Evolution of heavy minerals within present and Pliocene-Quaternary bedforms of the Moroccan Atlantic shelf and coast. *Bull. Inst. Géol. Bassin Aquitaine*, **43,** 153–161.

Bouma, A.H. (1962) *Sedimentology of Some Flysch Deposits.* Elsevier, Amsterdam, 168 pp.

Damuth, J.E. and **Flood, R.D.** (1985) Amazon Fan, Atlantic Ocean. In: *Submarine Fans and Related Turbidite Systems* (Eds A.H. Bouma, W.R. Normark and N.E. Barnes), pp. 97–106. Springer-Verlag, New York.

Davies, T.L. (1995) Turbidity Current Processes and High-resolution Stratigraphy for the Seine Abyssal Plain, NW Africa. Unpubl. PhD Thesis. University of Wales, Cardiff, 158 pp.

Davies, T.L., van Niel, B., Kidd, R.B. and **Weaver, P.P.E.** (1997) Erosional characteristics and turbidity current links between the Seine and Madeira Abyssal Plain turbidites calculated from reworked coccolith assemblages. *Geo-Mar. Lett.*, **17,** 147–153.

Droz, L., Rigaut, F., Cochonat, P. and **Tofani, R.** (1996) Morphology and recent evolution of the Zaire turbidite system (Gulf of Guinea). *Geol. Soc. Am. Bull.*, **108,** 253–269.

Emmel, F.J. and Curray, J.R. (1985) Bengal Fan, Indian Ocean. In: *Submarine Fans and Related Turbidite Systems* (Ed. A.H. Bouma, W.R. Normark and N.E. Barnes), pp. 107–112. Springer-Verlag, New York.

Ercilla, G., Alonso, B., Perez-Belzuz, F., Estrada, F., Baraza, J., Farran, M., Canals, M. and **Masson, D.** (1998) Origin, sedimentary processes and depositional evolution of the Agadir turbidite system (Central Eastern Atlantic). *J. Geol. Soc. London*, **155,** 929–939.

Gardner, J.V., Prior, D.B. and **Field, M.E.** (1999) Humboldt Slide – a large shear-dominated retrogressive slope failure. *Mar. Geol.*, **154,** 323–338.

Griffiths, J.F. (1972) *Climates of Africa: World Survey of Climatology*, **Vol. 10**. Elsevier, Amsterdam, 604 pp.

Heezen, B.C., Tharp, M. and **Ewing, M.** (1959) The floors of the oceans. *Geol. Soc. Am. Spec. Paper*, **65,** 122–137.

Hesse, R., Chough, S.K. and **Rakofsky, A.** (1987) The Northwest Atlantic Mid-Ocean Channel of the Labrador Sea. V. Sedimentology of a giant deep sea channel. *Can. J. Earth Sci.*, **24,** 1595–1624.

Hesse, R., Klaucke, I., Ryan, W.B.F., Edwards, M.B. and **Piper, D.J.W.** (1996) Imaging Laurentide Ice Sheet drainage into the deep sea: impact on sediments and bottom water. *Geol. Soc. Am. Today*, **6,** 3–9.

Jaaidi, El, B. and **Cirac, P.** (1987) The unconsolidated sedimentary blanket of the Moroccan Atlantic continental shelf between Larache and Agadir. *Bull. Inst. Géol. Bassin Aquitaine*, **42,** 35–51.

Kneller, B. (1995) Beyond the turbidite paradigm: physical models for deposition of turbidites and their implications for reservoir prediction. In: *Characterisation of Deep Marine Clastic Systems* (Eds A.J. Hartley and D.J. Prosser), *Geol. Soc. London Spec. Publ.*, 94, 31–49.

Kolla, V. and **Coumes, F.** (1985) Indus Fan, Indian Ocean. In: *Submarine Fans and Related Turbidite Systems* (Eds A.H. Bouma, W.R. Normark and N.E. Barnes), pp. 129–136. Springer-Verlag, New York.

de Lange, G.J., Jarvis, I. and **Kuijpers, A.** (1987) Geochemical characteristics and provenance of late Quaternary sediments from the Madeira Abyssal Plain, North Atlantic. In: *Geology and Geochemistry of Abyssal Plains* (Eds P.P.E. Weaver and J. Thomson), *Geol. Soc. London Spec. Publ.*, 31, 147–165.

Laughton, A.S. (1960) An interplain deep sea channel system. *Deep Sea Res.*, **7,** 75–88.

Lewis, K.B. (1994) The 1500 km long Hikurangi Channel: trench-axis channel that escapes its trench, crosses a plateau, and feeds a fan drift. *Geo-Mar. Lett.*, **14,** 19–28.

Lowe, D.R. (1982) Sediment gravity flows. II. Depositional models with special reference to the deposits of high-density turbidity currents. *J. Sed. Petrol.*, **52,** 279–297.

McMaster, R.L. and **Lachance, T.P.** (1969) Northwest African continental shelf sediments. *Mar. Geol.*, **7,** 57–67.

Martinson, D.G., Pisas, N.G., Hays, J.D., Imbrie, J., Moore, T.C. and **Shackleton, N.J.** (1987) Age dating and the orbital theory of the ice ages; development of a high resolution 0–300,000 year chronostratigraphy. *Quatern. Res.*, **27,** 1–29.

Masson, D.G. (1994) Late Quaternary turbidity current pathways to the Madeira Abyssal Plain and some constraints on turbidity current mechanisms. *Basin Res.*, **6,** 17–33.

Masson, D.G., Kidd, R.B., Gardner, J.V., Huggett, Q.J. and **Weaver, P.P.E.** (1992) Saharan Continental Rise: Facies Distribution and Sediment Slides. In: *Geologic Evolution of Atlantic Continental Rises* (Eds C.W. Poag and P.C. de Graciansky), pp. 327–346. Reinhold, Berlin.

Pearce, T.J. and **Jarvis, I.** (1992) Composition and provenance of turbidite sands: Late Quaternary, Madeira Abyssal Plain. *Mar. Geol.*, **109,** 21–51.

Piper, D.J.W. (1978) Turbidite muds and silts on deep-sea fans and abyssal plains. In: *Sedimentation in Submarine Canyons, Fans and Trenches* (Eds D.J. Stanley and G. Kelling), pp. 163–176. Dowden, Hutchinson & Ross, Stroudsburg.

Piper, D.J.W., Stow, D.A.V. and **Normark, W.R.** (1984) The Laurentian Fan; Sohm Abyssal Plain. *Geo-Mar. Lett.*, **3,** 141–146.

Reading, H.G. and **Richards, M.** (1994) Turbidite systems in deep-water basin margins classified by grain size and feeder systems. *AAPG Bull.*, **78,** 792–822.

Robinson, S.G. (1993) Lithostratigraphic applications for magnetic susceptibility logging of deep-sea sediment cores: examples from ODP Leg 115. In. *High Resolution Stratigraphy* (Eds E.A. Hailwood and R.B. Kidd), *Geol. Soc. London Spec. Publ.*, 70, 65–98.

Rothwell, R.G. (1989) *Minerals and Mineraloids in Marine Sediments: an Optical Identification Guide.* Elsevier, London, 279 pp.

Rothwell, R.G., Pearce, T.J. and **Weaver, P.P.E.** (1992) Late Quaternary evolution of the Madeira Abyssal Plain, Canary Basin, NE Atlantic. *Basin Res.*, **4,** 103–131.

Searle, R.C. (1987) Regional setting and geophysical characterisation of the Great Meteor East area in the Madeira Abyssal Plain. In: *Geology and Geochemistry of Abyssal Plains* (Eds P.P.E. Weaver and J. Thomson), *Geol. Soc. London Spec. Publ.*, 31, 49–70.

Shanmugam, G. and **Moiola, R.J.** (1981) Eustatic control of turbidites and winnowed turbidites. *Geology*, **10,** 231–235.

Stow, D.A.V. (1985) Deep-sea clastics. Where are we and where are we going? In: *Sedimentology, Recent Developments and Applied Aspects* (Eds P.J. Brenchley and B.P.J. Williams), *Geol. Soc. London Spec. Publ.*, 18, 67–93.

Stow, D.A.V. and **Shanmugam, G.** (1980) Sequence of structures in fine-grained turbidites: comparison of recent deep sea and ancient flysch sediments. *Sed. Geol.*, **25,** 23–42.

Stow, D.A.V., Howell, D.G. and **Nelson, C.H.** (1984) Sedimentary, tectonic and sea-level controls on submarine fans and slope-apron turbidite systems. *Geo-Mar. Lett.*, **3,** 57–64.

Summerhayes, C.P., Milliman, J.D., Briggs, S.R., Bee, A.G. and **Hogan, C.** (1976) Northwest African shelf sediments: influence of climate and sedimentary processes. *J. Geol.*, **84,** 277–300.

Thierstein, H.R., Geitzenauer, K.R., Molfino, B. and **Shackleton, N.J.** (1977) Global synchroneity of Late Quaternary coccolith datum levels: validation by oxygen isotopes. *Geology*, **5,** 400–404.

Thomson, J. and **Weaver, P.P.E.** (1994) An AMS radiocarbon method to determine the emplacement time of recent deep-sea turbidites. *Sed. Geol.*, **89,** 1–7.

Weaver, P.P.E. (1983) An integrated stratigraphy of the upper Quaternary of the King's Trough Flank area, N.E. Atlantic. *Oceanol. Acta*, **6,** 451–456.

Weaver, P.P.E. (1993) High resolution stratigraphy of marine Quaternary sequences. In: *High Resolution Stratigraphy* (Eds E.A. Hailwood and R.B. Kidd), *Geol. Soc. London Spec. Publ.*, 70, 137–153.

Weaver, P.P.E. (1994) Determination of turbidity current erosional characteristics from reworked coccolith assemblages, Canary Basin, north-east Atlantic. *Sedimentology*, **41,** 1025–1038.

Weaver, P.P.E. and **Kuijpers, A.** (1983) Climatic control of turbidite deposition on the Madeira Abyssal Plain. *Nature*, **306,** 360–363.

Weaver, P.P.E. and **Rothwell, R.G.** (1987) Sedimentation on the Madeira Abyssal Plain over the last 300,000 years. In. *Geology and Geochemistry of Abyssal Plains* (Eds P.P.E. Weaver and J. Thomson), *Geol. Soc. London Spec. Publ.*, 31, 71–86.

Weaver, P.P.E., Rothwell, R.G., Ebbing, J., Gunn, D. and **Hunter, P.M.** (1992) Correlation, frequency of emplacement and source directions of megaturbidites on the Madeira Abyssal Plain. *Mar. Geol.*, **109,** 1–20.

Weaver, P.P.E., Jarvis, I., Lebreiro, S.M., Alibes, B., Baraza, J., Howe, R. and **Rothwell, R.G.** (1998) The Neogene turbidite sequence on the Madeira Abyssal Plain: basin filling and diagenesis in the deep ocean. In: *Proceedings of the ODP Sci. Results 157* (Eds P.P.E. Weaver, H.-U. Schmincke, J.V. Firth and W. Duffield). pp. 619–634. Ocean Drilling Program, College Station, TX.

Weaver, P.P.E., Wynn, R.B., Kenyon, N.H. and **Evans, J.** (2000) Continental margin sedimentation, with special reference to the north-east Atlantic margin. *Sedimentology*, **47** (Suppl. 1), 239–256.

Wynn, R.B., Masson, D.G., Stow, D.A.V. and **Weaver, P.P.E.** (2000) The Northwest African slope apron: a modern analogue for deep-water systems with complex seafloor topography. *Mar. Petrol. Geol.*, **17,** 253–265.

Wynn, R.B., Stow, D.A.V., Kenyon, N.H., Masson, D.G. and **Weaver, P.P.E.** (2002) A new model for channel termination zones based on high-resolution sidescan sonar and modern and ancient analogues. *AAPG Bull.*, (in press).

Zaragosi, S., Auffret, G.A., Faugeres, J.-C., Garlan, T., Pujol, C. and **Cortijo, E.** (2000) Physiography and recent sediment distribution of the Celtic Deep-Sea Fan, Bay of Biscay. *Mar. Geol.*, **169,** 207–237.

Manuscript received 25 July 2000;
revision accepted 24 February 2002.